

ChemistrySelect

Chemistry  
Europe  
European Chemical  
Societies Publishing

## Editorial Board

## Chairs



**Didier Astruc** is a full professor of chemistry at the Université Bordeaux I. He is known for his work on "electron-reservoir" complexes, dendritic molecular batteries, green catalysis, and sensors.



**Hélène Lebel** is a professor of chemistry at the Université de Montréal. Her research is focused on catalysis in synthetic organic chemistry, pharmacologically useful molecules, and multicatalytic processes that mimic biosynthesis in living cells.



**An-Hui Lu** is a professor of chemistry at the State Key Laboratory of Fine Chemicals, Dalian University of Technology. His research interests include the synthesis of porous materials for heterogeneous catalysis, adsorption, energy storage and conversion.







## Members

- Raed Abu-Reziq** (The Hebrew University of Jerusalem)
- Marius Andruh** (Universitatea din București)
- Ülkü Anık** (Muğla Sıtkı Koçman University)
- Viktorya Aviyente** (Boğaziçi University)
- R. Tom Baker** (University of Ottawa)
- Thomas Baumgartner** (York University)
- Michael J. Bojdys** (Humboldt-Universität zu Berlin)
- Azzedine Bousseksou** (Laboratoire de Chimie de Coordination, CNRS)
- Carlos D. Brondino** (Universidad Nacional del Litoral)
- Juraj Bujdak** (Univerzita Komenského v Bratislave)
- Jianfeng Cai** (University of South Florida)
- Luigi Cavallo** (King Abdullah University of Science and Technology)
- Jiří Čejka** (Akademie věd České republiky)
- Hugo E. Cerecetto** (Universidad de la República)
- Banglin Chen** (University of Texas at San Antonio)
- Sheng Dai** (Oak Ridge National Laboratory)
- Jiří Damborský** (Masarykova univerzita)
- Aditi Das** (University of Illinois)
- Fabian M. Dayrit** (Ateneo de Manila University)
- Da-Ming Du** (Beijing Institute of Technology)
- Charl Faul** (University of Bristol)
- Shin-ichi Fukuzawa** (Chuo University)
- François Gabbai** (Texas A&M University)
- Miran Gaberšček** (Kemijski inštitut Ljubljana Slovenija)
- Karol Grela** (University of Warsaw)
- Daniel Gryko** (Polska Akademia Nauk)
- Michael Harmata** (University of Missouri-Columbia)
- Christian Heinis** (École Polytechnique Fédérale de Lausanne)
- Dennis Hettterscheid** (Universiteit Leiden)

-  Yong-Sheng **Hu** (Institute of Physics, CAS)
-  Reuben **Hwu** (National Tsing Hua University)
-  Josef **Jampilek** (Univerzita Komenského v Bratislave)
-  Hye-Young **Jang** (Ajou University)
-  Knud **Jensen** (Københavns Universitet)
-  Deborah **Jones** (L'Institut de Chimie Moléculaire et des Matériaux)
-  Babak **Karimi** (Institute for Advanced Studies in Basic Sciences)
-  Uwe **Karst** (Westfälische Wilhelms-Universität Münster)
-  Henryk **Kozłowski** (Uniwersytet Wrocławski)
-  Yuehe **Lin** (Washington State University)
-  Chenghui **Liu** (Shaanxi Normal University)
-  Chun-yan **Liu** (Technical Institute of Physics and Chemistry, CAS)
-  Gregor **Mali** (Kemijski inštitut Ljubljana Slovenija)
-  Jose L. **Marco-Contelles** (Química Orgánica General del CSIQ)
-  Sherri **McFarland** (University of North Carolina at Greensboro)
-  Gabriel **Merino** (Centro de Investigación y de Estudios Avanzados Unidad Mérida)
-  Kenji **Miyatake** (University of Yamanashi)
-  Yirong **Mo** (Western Michigan University)
-  Thomas E. **Müller** (RWTH Aachen)
-  Samir H. **Mushrif** (University of Alberta)
-  Srinivasan **Natarajan** (Indian Institute of Science, Bangalore)
-  Georgii I. **Nikonov** (Brock University)
-  Turan **Öztürk** (Istanbul Technical University)
-  Mario **Pagliaro** (Istituto per lo Studio dei Materiali Nanostrutturati del CNR, Palermo)
-  Maurizio **Peruzzini** (Dipartimento Scienze Chimiche e Technologie del CNR)
-  Teresa M. V. D. **Pinho e Melo** (Universidade De Coimbra)
-  Uwe **Pischel** (Universidad de Huelva)
-  László **Poppe** (Budapesti Műszaki és Gazdaságtudományi Egyetem)
-  Vinich **Promarak** (Vidyasirimedhi Institute of Science and Technology)
-  Rasmita **Raval** (University of Liverpool)
-  Leni **Ritmaleni** (Universitas Gadjah Mada)
-  Johan **Rosengren** (The University of Queensland)
-  Liane Marcia **Rossi** (Universidade de São Paulo)
-  Agnieszka **Ruppert** (Politechnika Łódzka)
-  Ulrich **Schatzschneider** (Julius-Maximilians-Universität Würzburg)
-  YuYe Jay **Tong** (Georgetown University)
-  Konstantinos S. **Triantafyllidis** (Aristotle University of Thessaloniki)
-  Andrew **Tsotinis** (University of Athens)
-  Xinchun **Wang** (Fuzhou University)
-  Gang **Wu** (University at Buffalo)

## Former Members

-  Gaoquan **Shi** (Tsinghua University)

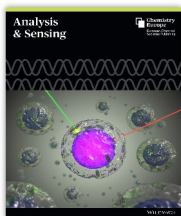
-  [Submit a Manuscript](#)
-  [Browse free sample issue](#)
-  [Get content alerts](#)
-  [Subscribe to this journal](#)

## More from this journal

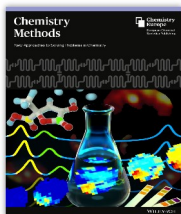
- [Reviews](#)
- [Editorials](#)
- [Video Abstracts](#)



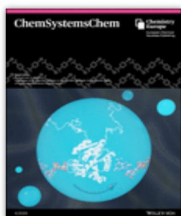




NEW JOURNAL:  
**Analysis & Sensing**  
Accepting submissions now.



NEW JOURNAL:  
**Chemistry—Methods**  
Accepting submissions now.



ISSUE  
Volume 2, Issue 4  
July 2020



ISSUE  
Volume 26, Issue 43  
Pages: 9403-9651  
August 3, 2020

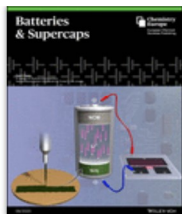


ISSUE  
Volume 9, Issue 8  
Pages: 793-817  
August 2020

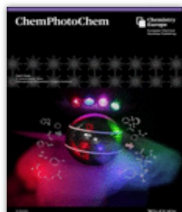


ISSUE  
Volume 5, Issue 29  
Pages: 8881-9312  
August 7, 2020

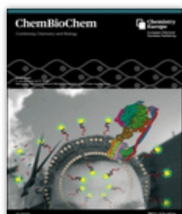




ISSUE  
Volume 3, Issue 8  
Pages: 668-788  
August 2020



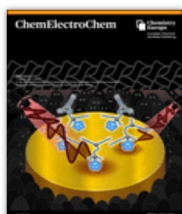
ISSUE  
Volume 4, Issue 7  
Pages: 451-534  
July 2020



ISSUE  
Volume 21, Issue 15  
Pages: 2086-2224  
August 3, 2020



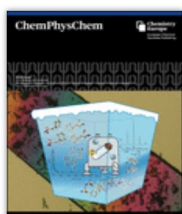
ISSUE  
Volume 12, Issue 14  
Pages: 3598-3792  
July 21, 2020



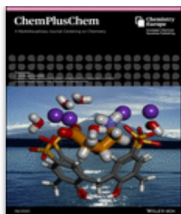
ISSUE  
Volume 7, Issue 15  
Pages: 3168-3323  
August 3, 2020



ISSUE  
Volume 15, Issue 15  
Pages: 1372-1496  
August 5, 2020



ISSUE  
Volume 21, Issue 15  
Pages: 1617-1736  
August 4, 2020



## ISSUE

Volume 85, Issue 8  
Pages: 1612-1709  
August 2020



## ISSUE

Volume 13, Issue 14  
Pages: 3539-3725  
July 22, 2020



## ISSUE

Volume 2020, Issue 29  
Pages: 2767-2849  
August 9, 2020



## ISSUE

Volume 2020, Issue 29  
Pages: 4433-4638  
August 9, 2020



[ChemistryViews.org](https://chemistryviews.org) Home

## Mn-Catalyzed Transfer Hydrogenation of Esters

06 Aug 2020

Ester reduction using ethanol instead of hydrogen

## 90th Anniversary: Death of Joseph Achille Le Bel

06 Aug 2020

French chemist and co-discoverer of the basic concepts of organic stereochemistry

## Giant Mo<sub>240</sub> Dodecahedra

05 Aug 2020

Polymolybdate cage with pentagonal openings

## Oxygen-Stable State of [FeFe] Hydrogenase Studied

05 Aug 2020

A sulfur ligand causes oxygen stability

## Nursing, Gut Bacteria, and the Immune System – Part 2

04 Aug 2020

What are human milk oligosaccharides (HMO)?

# ACES Asian Chemical Editorial Society



ISSUE

Volume 15, Issue 15

The Chemistry of 2D Materials Membranes

Pages: 2239-2378

August 3, 2020



ISSUE

Volume 9, Issue 7

Pages: 967-1086

July 2020



ISSUE

Volume 6, Issue 7

Pages: 996-1135

July 2020

© 2020 WILEY-VCH Verlag GmbH & Co. KGaA, Weinheim

About Wiley Online Library

[Privacy Policy](#)

[Terms of Use](#)

[Cookies](#)

[Accessibility](#)

[Help & Support](#)

[Contact Us](#)

[Opportunities](#)



**Subscription Agents**  
**Advertisers & Corporate Partners**

Connect with Wiley

**The Wiley Network**  
**Wiley Press Room**

Copyright © 1999-2020 John Wiley & Sons, Inc. All rights reserved

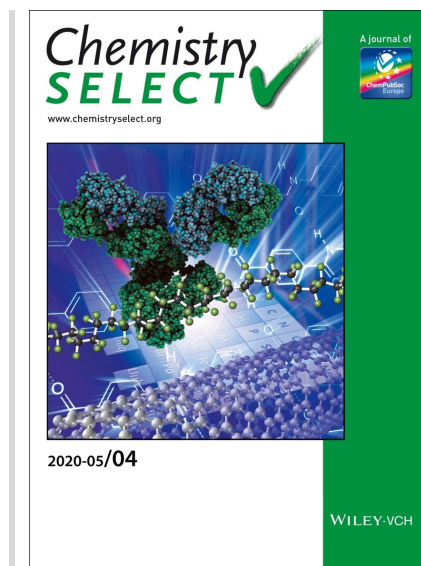
**ChemistrySelect****Chemistry  
Europe**  
European Chemical  
Societies Publishing**Volume 5, Issue 4**

Pages: 1247-1606

January 31, 2020

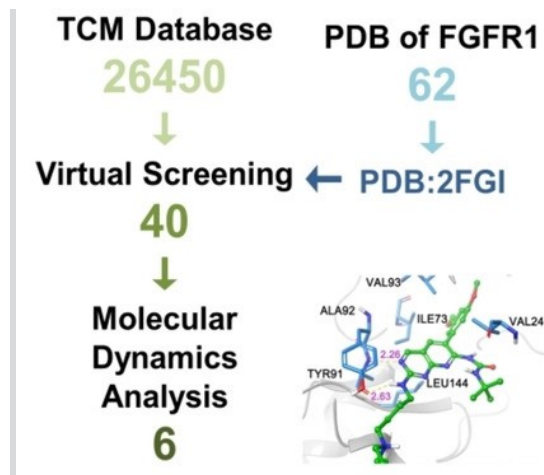
[< Previous Issue](#) | [Next Issue >](#) **GO TO SECTION****” Export Citation(s)****Cover Pictures** [Free Access](#)**Cover Picture: (04/2020)**

Pages: 1247 | First Published: 24 January 2020

[Abstract](#) | [PDF](#) | [Request permissions](#)**Full Papers****Medicinal Chemistry & Drug Discovery****Identification of Potential Inhibitors from Traditional Chinese Medicine for Fibroblast Growth Factor Receptor 1 Based on Virtual Screening and Molecular Dynamics Analysis**

Peng Sun, Chen Jiang, Dr. GuiFen Zhou, Prof. Qiao Yan Zhang, Dr. Gang Cheng, Prof. LuPing Qin

Pages: 1248-1254 | First Published: 24 January 2020



Fibroblast growth factor receptor 1 is a potential therapeutic target for osteoporosis and other diseases. In this study, we aim to identify FGFR1 inhibitors from Traditional Chinese Medicine (TCM) database. 26450 compounds were filtered by virtual screening to afford 40 potential compounds. And 6 candidates were selected based on molecular dynamics analysis of the with FGFR1 protein. Our modelling study would provide some clues to the discovery of novel FGFR1 inhibitors as potential therapeutic drugs.

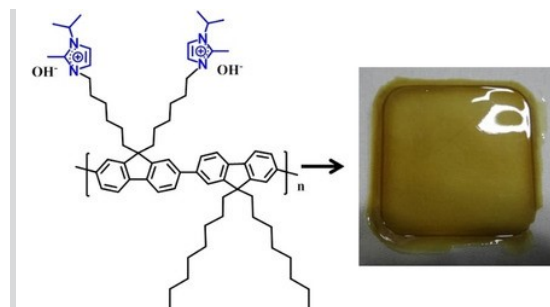
[Abstract](#) | [Full text](#) | [PDF](#) | [References](#) | [Request permissions](#)

## Materials Science inc. Nanomaterials & Polymers

### Imidazolium-Functionalized Fluorene-Based Anion Exchange Membrane (AEM) for Fuel Cell Applications

Umme Salma, Dishen Zhang, Dr. Yuki Nagao

Pages: 1255-1263 | First Published: 24 January 2020



Polyfluorene polymer with alkyl imidazolium cationic groups was newly synthesized. Membranes exhibited high  $\text{OH}^-$  conductivity and good thermal stability. Lower water uptake suppressed dimensional expansion of the membrane. Imidazolium groups degraded in highly alkaline media but the fluorene backbone remained chemically stable. We discussed discrepancies presented in the relevant literature.

[Abstract](#) | [Full text](#) | [PDF](#) | [References](#) | [Request permissions](#)

## Biological Chemistry & Chemical Biology

### “Turn-On” Sensing Behaviour of an In Situ Generated Fluorescein-Based Probe and Its Preferential Selectivity of Sodium Hypochlorite over *tert*-Butyl Hydroperoxide in Lung Adenocarcinoma Cells”

Navjot Sandhu, Sheetanshu Sapru, Dr. Srivatsava Naidu, Dr. Atul P. Singh, Dr. Kamlesh Kumar, Dr. Ashish P. Singh, Dr. Rajesh K. Yadav

Pages: 1264-1268 | First Published: 24 January 2020

With fluorescein-based probe F, *t*-BuOOH shows its unprecedented reducing behavior with “turn-off” sensing, while in-situ generated probe A by the reaction of *t*-BuOOH with Probe F, shows “turn-on” sensing property with NaOCl.

[Abstract](#) | [Full text](#) | [PDF](#) | [References](#) | [Request permissions](#)

## Organic & Supramolecular Chemistry

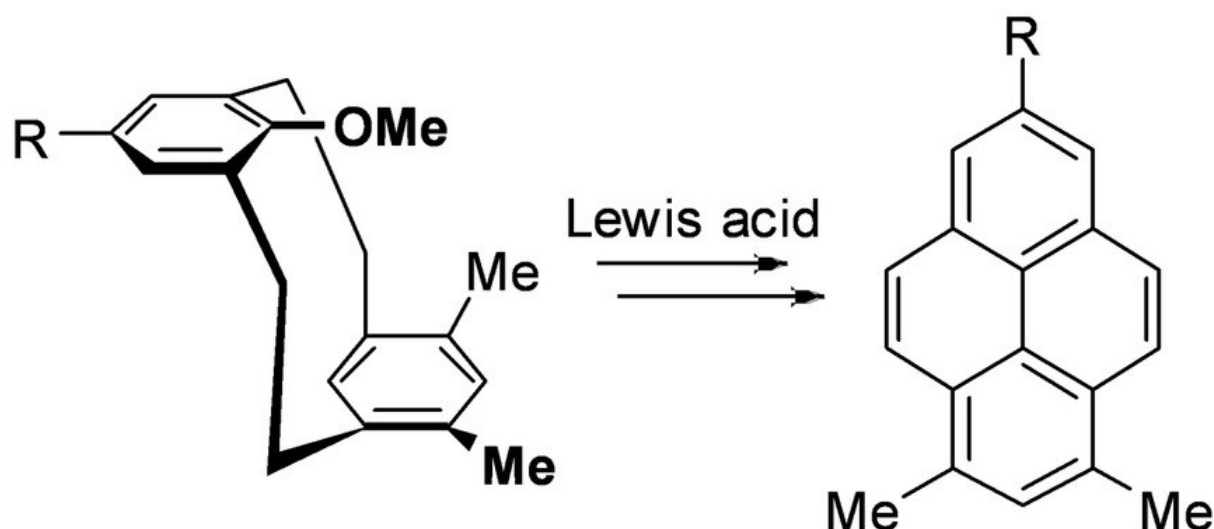
### Studies on Lewis-Acid Induced Reactions of 8-Methoxy[2.2]metacyclophanes: A New Synthetic Route to Alkylated Pyrenes

Dr. Md. Monarul Islam, Dr. Xing Feng, Dr. Chuan-Zeng Wang, Dr. Shofiur Rahman, Dr. Abdullah Alodhayb, Dr. Prof. Paris E. Georgiou, Dr. Taisuke Matsumoto, Dr. Junji Tanaka, Prof. Dr. Carl Redshaw, Dr. Prof. Takehiko Yamato



Pages: 1269-1274 | First Published: 24 January 2020

Probe F + 45 eq. NaOCl



A simple and effective method for the synthesis of [2.2]metacyclophanes, and Lewis acid induced transannular reactions leading also to new alkylated pyrenes is reported along with a DFT computational study.

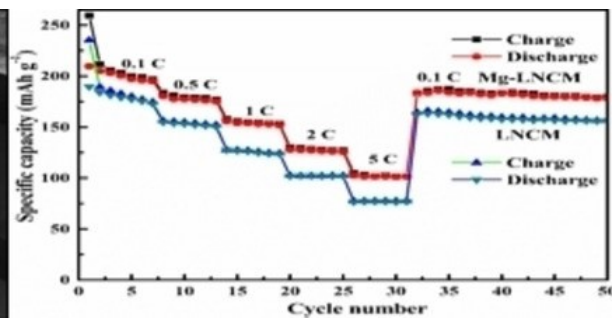
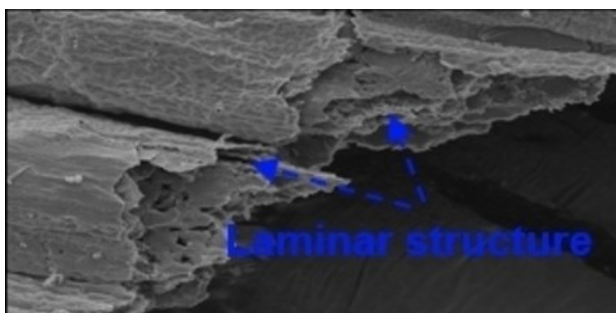
[Abstract](#) | [Full text](#) | [PDF](#) | [References](#) | [Request permissions](#)

## Inorganic Chemistry

### Mg<sup>2+</sup> Doped LiNi<sub>1/3</sub>Co<sub>1/3</sub>Mn<sub>1/3</sub>O<sub>2</sub> Hollow Flake-Like Structures with Enhanced Performances Cathodes for Lithium-Ion Batteries

Qiangchao Sun, Hongwei Cheng, Kangning Zhao, Huijie Zhou, Hongbin Zhao, Wenli Yao, Qian Xu, Xiongqiang Lu

Pages: 1275-1281 | First Published: 24 January 2020



We reported the Mg-doped hollow flake-like fiber LiNi<sub>1/3</sub>Co<sub>1/3</sub>Mn<sub>1/3</sub>O<sub>2</sub> cathodes with improved electrochemical performances were successfully synthesized by cost-effective raw materials and facile fabricate method. The Li (Ni<sub>1/3</sub>Co<sub>1/3</sub>Mn<sub>1/3</sub>)<sub>0.99</sub>Mg<sub>0.01</sub>O<sub>2</sub> cathode materials exhibit desirable high rate capability and improved cycling stability compared to the pristine LiNi<sub>1/3</sub>Co<sub>1/3</sub>Mn<sub>1/3</sub>O<sub>2</sub> cathodes. The synergy of element doping and micro-structural regulation could facilitate the application of LiNi<sub>1/3</sub>Co<sub>1/3</sub>Mn<sub>1/3</sub>O<sub>2</sub> cathode materials in high energy and power densities lithium ion batteries fields.

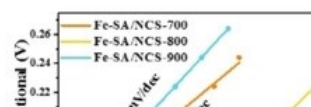
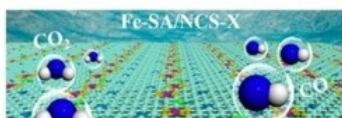
[Abstract](#) | [Full text](#) | [PDF](#) | [References](#) | [Request permissions](#)

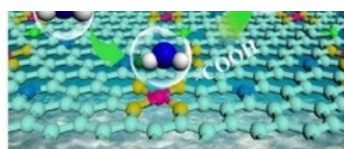
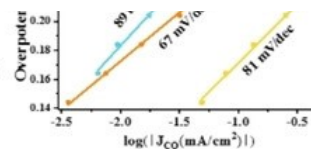
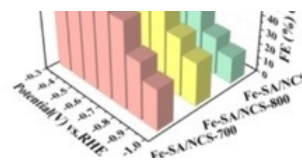
## Catalysis

### Single-Atom Iron-Nitrogen Catalytic Site with Graphitic Nitrogen for Efficient Electroreduction of CO<sub>2</sub>

Dr. Ying Zhu, Dr. Xueyan Li, Dr. Xingpu Wang, Dr. Kuilin Lv, Dr. Guozheng Xiao, Jingjing Feng, Xiaohui Jiang, Mingwei Fang, Prof. Ying Zhu

Pages: 1282-1287 | First Published: 24 January 2020



CO<sub>2</sub>RR Performance

A single-atom Fe dispersed on N-doped carbon nanosheets (Fe-SA/NCS-X) with high activity and selectivity for CO<sub>2</sub> electroreduction to CO was designed and developed by pyrolyzing precursor of hemin-doped polyaniline.

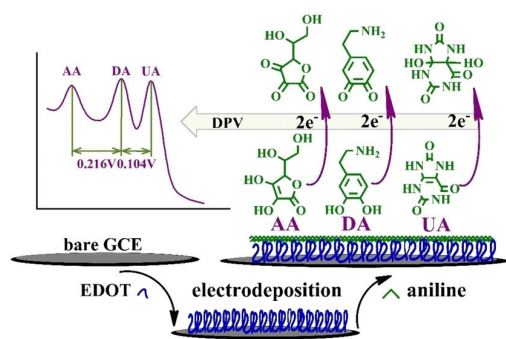
[Abstract](#) | [Full text](#) | [PDF](#) | [References](#) | [Request permissions](#)

## Analytical Chemistry

### Electrodeposition of Three-Dimensional Network Nanostructure PEDOT/PANI for Simultaneous Voltammetric Detection of Ascorbic Acid, Dopamine and Uric Acid

Qiangwei Wang, Haobo Sun, Qianrui Liu, Prof. Lianzhi Li, Prof. Jinming Kong

Pages: 1288-1293 | First Published: 24 January 2020



Three-dimensional network structure PEDOT/PANI was electrodeposited on GCE; Ascorbic acid, dopamine and uric acid are oxidized on the surface of GCE/PEDOT/PANI at different oxidation potentials.

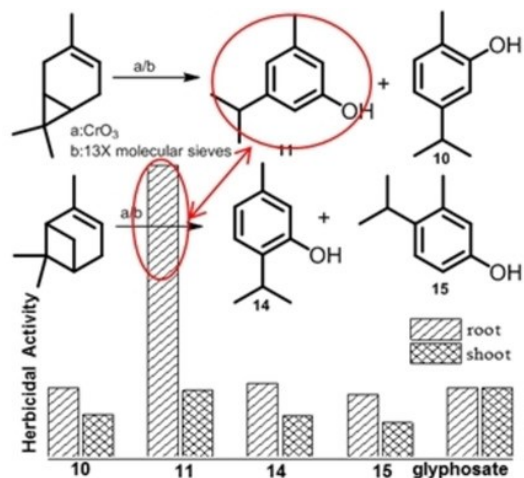
[Abstract](#) | [Full text](#) | [PDF](#) | [References](#) | [Request permissions](#)

## Sustainable Chemistry

### Isopropyl Cresols: Synthesis and Herbicidal Activity

Jing Wang, Huanhuan Dong, Hongmei Zhang, Songlin Dai, Prof. Jianxin Jiang, Prof. Zhendong Zhao

Pages: 1294-1299 | First Published: 24 January 2020



Four isopropyl cresols were prepared from two monoterpenes by a simple process. The herbicidal activity of 5-isopropyl-3-methylphenol (**11**) was considerably higher than those of glyphosate and the isomers **10**, **14**, and **15** toward the root growth of barnyard grass.

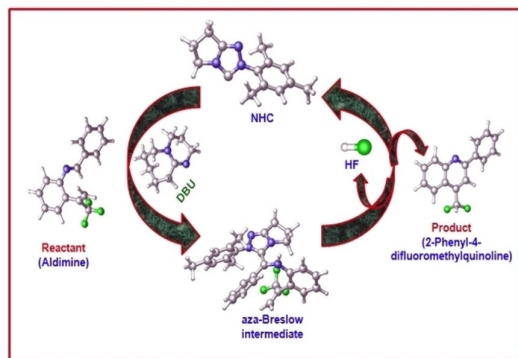
[Abstract](#) | [Full text](#) | [PDF](#) | [References](#) | [Request permissions](#)

## Catalysis

## Theoretical Insight towards Mechanism, Role of NHC and DBU in the Synthesis of Substituted Quinolines

Abhijit Shyam, Prof. Paritosh Mondal

Pages: 1300-1307 | First Published: 24 January 2020



A detail mechanistic investigation on N-heterocyclic carbene (NHC) catalyzed synthesis of 2-phenyl-4-difluoromethylquinoline from aldimine has been performed by using density functional theory (DFT) method. The proposed catalytic cycle is found to be comprised of six significant stages through the formation of an aza-Breslow intermediate. Catalyst NHC and the base 1,8-diazabicyclo[5.4.0]undec-7-ene (DBU) have been cooperatively participated to accomplish this reaction efficiently.

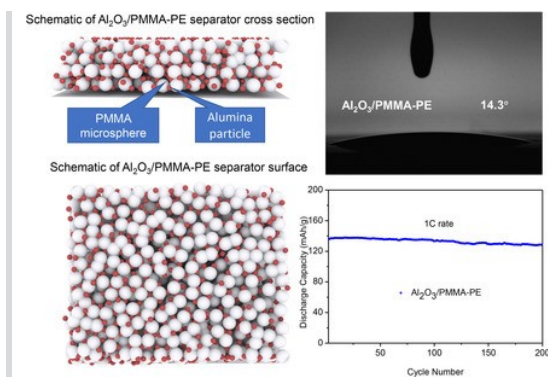
[Abstract](#) | [Full text](#) | [PDF](#) | [References](#) | [Request permissions](#)

## Materials Science inc. Nanomaterials & Polymers

### Organic-Inorganic Composite Porous Membrane for Stable and High-Performance Lithium-Ion Battery

Dr. Wen Lin, Dr. Jiajia Jiao, Dr. Hao Li, Dr. Danpeng Li, Dr. Taiyang Zhu, Dr. Jiangping Song, Dr. Shenqiu Zhao, Dr. Weibin Guo, Prof. Haolin Tang

Pages: 1308-1314 | First Published: 24 January 2020



In this paper, alumina and Poly (methyl methacrylate) microsphere organic-inorganic composite Porous membranes were prepared. The synergistic effect of alumina particles and Poly (methyl methacrylate) microspheres is used to improve the separator performance. Poly (methyl methacrylate) and alpha alumina are joined together by electrostatic interaction. Poly (methyl methacrylate) coating could improves electrolyte wettability. Besides, alpha alumina could reduce the expansion effect of Poly (methyl methacrylate) after absorbing electrolyte to improve cycle performance of lithium batteries.

[Abstract](#) | [Full text](#) | [PDF](#) | [References](#) | [Request permissions](#)

### Fabrication of Antibacterial Nanofibers Composites by Functionalizing the Surface of Cellulose Acetate Nanofibers

Dr. Muhammad Qamar Khan, Dr. Davood Kharaghani, Dr. Sanaullah, Dr. Amir Shahzad, Dr. Nam Phan Duy, Dr. Yohei Hasegawa, Dr. Azeemullah, Prof. Jungsoon Lee, Prof. Ick Soo Kim

Pages: 1315-1321 | First Published: 24 January 2020

The silver sulfadiazine (SSD) nanoparticles were successfully synthesized on the surface of cellulose acetate nanofibers web by in-situ facile method in which nanofibers webs were immersed in the solution of sodium sulfadiazine salt/silver nitrate ( $\text{AgNO}_3$ ). All characterization results supported that this composite can be used for antibacterial wound dressings due to excellent antibacterial properties against *gram negative E. coli*, which is unique properties of SSD for antibacterial activity.

[Abstract](#) | [Full text](#) | [PDF](#) | [References](#) | [Request permissions](#)

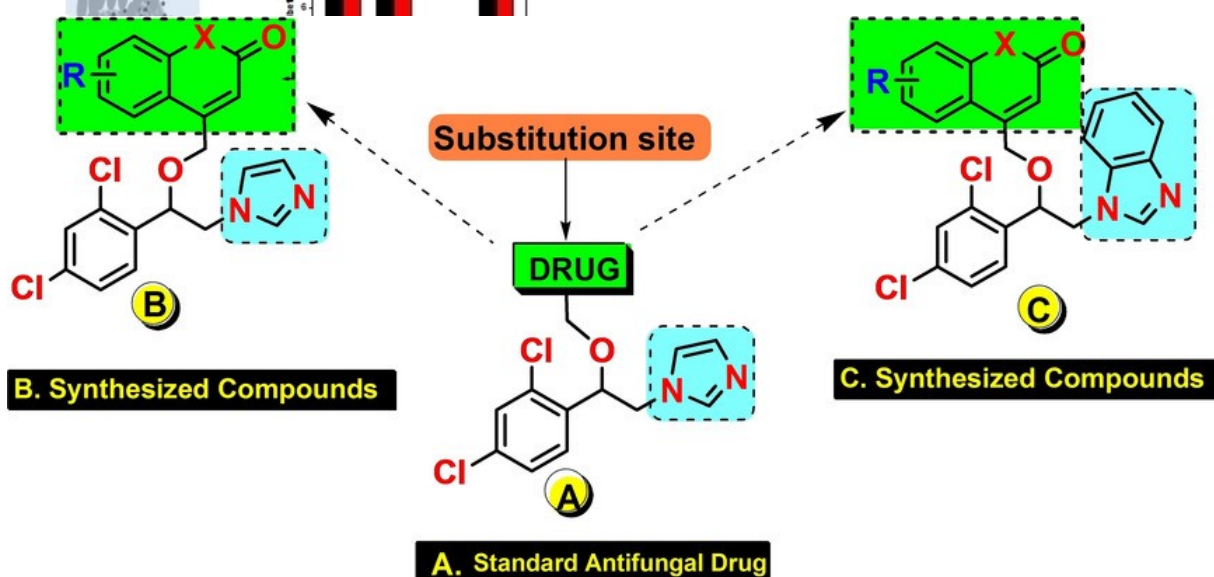
## Biological Chemistry & Chemical Biology

### Synthesis and Molecular Modelling Studies of Coumarin and 1-Aza-Coumarin Linked Miconazole Analogues and Their Antimicrobial Properties



Suraj M. Sutar, Hemantkumar M. Savanur, Shashikant S. Molunavar, Geeta M. Pawashe, Dr. Gopalakrishnan Aridoss, Dr. Kang Min Kim, Jin Young Lee, Dr. Rajesh G. Kalkhambkar

Pages: 1322-1330 | First Published: 30 January 2020



A series of coumarin, 1-Azacoumarin, Imidazole and benzimidazole linked miconazole analogue of compounds were synthesized by modification in the readily available miconazole moiety to screen it towards its antimicrobial properties. Molecular modelling studies found to be effective with excellent binding affinity results. Further, some of the synthesized compounds exhibited excellent antibacterial and antifungal activity compared to that of standard. Further.

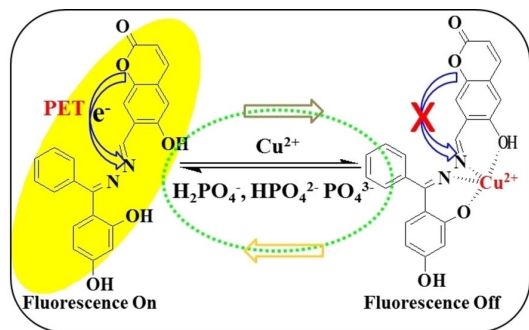
[Abstract](#) | [Full text](#) | [PDF](#) | [References](#) | [Request permissions](#)

## Analytical Chemistry

### A Dual-Functional "On-Off-On" Relay Fluorescent Probe for the Highly Sensitive Detection of Copper(II) and Phosphate Ions

Dr. Minmin Wang, Chun Wang, Prof. Miao Wang, Prof. Tongming Sun, Yang Huang, Prof. Yanfeng Tang, Jianfeng Ju, Lujie Shen, Yeyu Hu, Prof. Jinli Zhu

Pages: 1331-1334 | First Published: 24 January 2020



A dual-functional "On-Off-On" relay fluorescent probe for highly sensitive detect  $\text{Cu}^{2+}$  and phosphate ions was fabricated. The stoichiometric ratio of  $\text{L}-\text{Cu}^{2+}$  complex was determined as 1 : 1 based on  $^1\text{H}$  NMR titration and ESI-MS. The detection limit for  $\text{Cu}^{2+}$  was up to  $6.14 \times 10^{-7}$  M. Meanwhile, the complex of  $\text{L}-\text{Cu}^{2+}$  show a high response to  $\text{H}_2\text{PO}_4^-$ ,  $\text{HPO}_4^{2-}$  and  $\text{PO}_4^{3-}$  which denote the probe L a better "on-off-on" properties.

[Abstract](#) | [Full text](#) | [PDF](#) | [References](#) | [Request permissions](#)

## Reviews

### Materials Science inc. Nanomaterials & Polymers

#### A Review on the Secondary Surface Morphology of Electrospun Nanofibers: Formation Mechanisms, Characterizations, and Applications

Bilal Zaarour, Lei Zhu, Xiangyu Jin

Pages: 1335-1348 | First Published: 24 January 2020



This review article provides a comprehensive review on the secondary surface morphology of electrospun fibers (fibers without smooth surface and solid interior) such as porous structure, grooved structure, wrinkled structure, rough structure, cactus structure, and hollow structure. Basic principles about the electrospinning process, types of electrospinning, materials, formation mechanisms, characterizations, and applications of electrospun fibers with the secondary surface morphology are discussed in detail.

[Abstract](#) | [Full text](#) | [PDF](#) | [References](#) | [Request permissions](#)

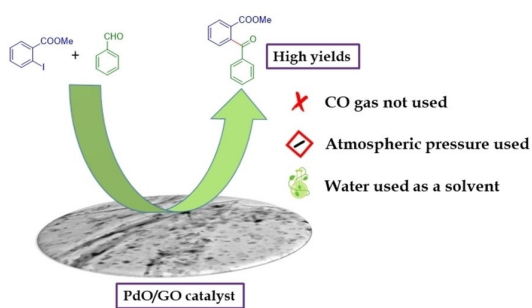
## Full Papers

### Organic & Supramolecular Chemistry

#### Heterogeneous Direct Acylation Strategy to Diaryl Ketones and Their Application to 1,3-Dihydroisobenzofurans

Trisha Bhattacharya, Basuli Suchand, Chinnabattigalla Sreenivasulu, Bhairi Lakshminarayana, Ch. Subrahmanyam, G. Satyanarayana

Pages: 1349-1352 | First Published: 24 January 2020



Aromatic acylation is an indispensable chemical transformation in organic synthesis in affording aryl ketones. In this manuscript, we have described the synthesis of aromatic ketones utilizing graphene oxide (GO) supported PdO nanoparticles (PdO/GO), as heterogeneous transition metal catalyst. The [Pd]-heterogeneous catalyst enabled the coupling between iodoarenes and aromatic aldehydes. The acylation was carried out by eliminating toxic CO gas as the source of the carbonyl. Further, practicality of this strategy was also demonstrated by fusing 1,3-dihydroisobenzofurans.

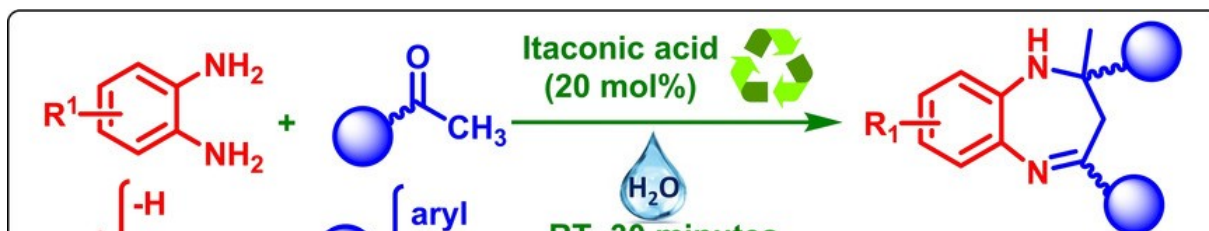
[Abstract](#) | [Full text](#) | [PDF](#) | [References](#) | [Request permissions](#)

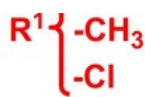
## Sustainable Chemistry

#### Recyclable Itaconic Acid with Water as Green Catalytic System: Synthesis of Substituted 1,5-Benzodiazepine Derivatives at Room Temperature

Kashyap J. Tamuli, Prof. Manobjyoti Bordoloi

Pages: 1353-1358 | First Published: 24 January 2020





RT, 30 minutes

**1,5-benzodiazepines**  
(61-95% yields)  
[32 examples]

■ Ketones, alkynes and chalcones as coupling partners ■ Metal-Free Approach  
■ Recyclable Catalyst ■ No Chromatography ■ Large Scale Synthesis

To reduce the use of toxic organic solvents by water, herein we have introduced itaconic acid as mild acid source to synthesized 1,5-benzodiazepine derivatives at room temperature in 30 minutes. After completion of the reaction, the aqueous part can be reused further for the synthesis of such *N*-containing heterocycles up to 5<sup>th</sup> cycle.

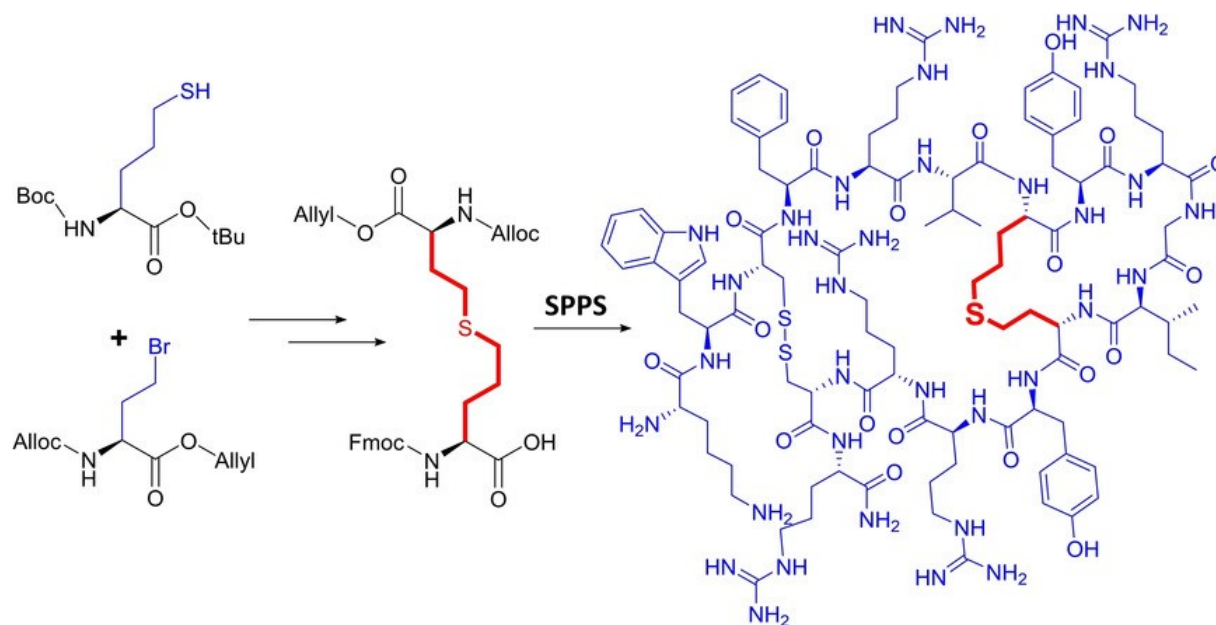
[Abstract](#) | [Full text](#) | [PDF](#) | [References](#) | [Request permissions](#)

## Biological Chemistry & Chemical Biology

### Chemical Synthesis of Six-Atom Thioether Bridged Diaminodiacid for Solid-Phase Synthesis of Peptide Disulfide Bond Mimics

Junyou Chen, Shuaishuai Sun, Rui Zhao, Chen-Peng Xi, Wenjie Qiu, Prof. Ning Wang, Dr. Ya Wang, Dr. Donald Bierer, Prof. Jing Shi, Prof. Yi-Ming Li

Pages: 1359-1363 | First Published: 24 January 2020



We successfully synthesized six-atom diaminodiacid for the first time, and the key unit can be efficiently prepared by a new method for converting a side chain carboxyl group into a thiol group. The diaminodiacid applied to synthesis TPI peptide analog. The utility of this diaminodiacid is demonstrated in the synthesis of tachyplesin disulfide analogues, which not only had good activity but also increased stability under reducing conditions.

[Abstract](#) | [Full text](#) | [PDF](#) | [References](#) | [Request permissions](#)

## Catalysis

### Addition of Ce in Cu/Three-Dimensional Graphene Derived from Watermelon for Low Temperature NH<sub>3</sub>-SCR

Yan Kang, Dr. Zhifang Li, Dr. Jinxing Cui, Cui Geng, Chao Zhang, Peng Li, Prof. Changlong Yang

Pages: 1364-1369 | First Published: 24 January 2020

A novel series of Cu-Ce modified three-dimensional structured graphene (3DG) from watermelon catalysts (Cu-Ce/3DG) were synthesized by the hydrothermal crystallization method for the selective catalytic reduction of NO<sub>x</sub> by NH<sub>3</sub>. The results showed that 2Cu-3Ce/3DG demonstrated excellent low-temperature SCR activity due to the increase of the Cu<sup>+</sup>, Ce<sup>3+</sup> and the form of the abundant acid sites. Furthermore, it displayed the good conversion rate of NO<sub>x</sub> in the presence of SO<sub>2</sub>.



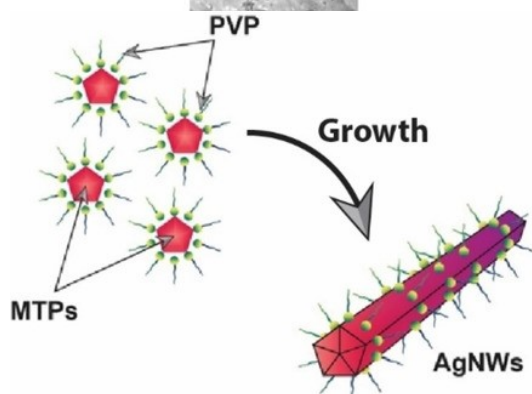
Abstract | Full text | PDF | References | Request permissions

Materials Science inc. Nanomaterials & Polymers

## All-solution Processed Highly Transparent Silver Nanowires/PEDOT:PSS Conducting Thin Films for Optoelectronic Applications

Mathew K Francis, Dr. Pankaj Balaji Bhargav, Nafis Ahmed, Balaji Chandra, Dr. Dhakshina Moorthy Gnanapraksh, Nivetha Thyagarajan, Ramamurthy Racchana

Pages: 1370-1374 | First Published: 24 January 2020



In this paper, silver nanowires (AgNWs) were synthesized using rapid synthesis polyol process by keeping polyvinylpyrrolidone (PVP): silver nitrate ( $\text{AgNO}_3$ ) ratio constant and their effect on the formation of AgNWs is systematically investigated. AgNWs with typical average length of  $5\ \mu\text{m}$  were grown at higher concentration of  $\text{AgNO}_3$  (0.08 M). A hybrid transparent conducting electrode (TCE) was fabricated by spin-coating a mix of optimized AgNWs in conducting polymer matrix-poly(3,4-ethylenedioxythiophene) polystyrene sulfonate (PEDOT:PSS) on to glass substrate.

Abstract | Full text | PDF | References | Request permissions

Energy Technology & Environmental Science

## Jatropha Oil Cake Based Activated Carbon for Symmetric Supercapacitor Application: A Comparative Study on Conventional and Hydrothermal Carbonization Processes

M. Siva Sankari, S. Vivekanandhan

Pages: 1375-1384 | First Published: 27 January 2020



The Jatropha oilcake was effectively converted into pristine and activated biocarbons employing conventional and hydrothermal carbonizations. Activation process enhanced the specific surface area of Jatropha oilcake based carbon materials, which showed higher specific surface area. The synthesized pristine and activated biocarbons were explored for supercapacitor applications. Activated biocarbon derived through hydrothermal carbonization showed highest specific capacity of 174.78 F/g.

Abstract | Full text | PDF | References | Request permissions

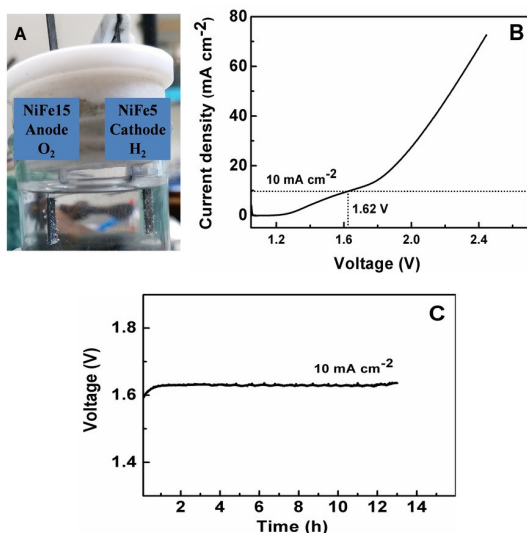
Catalysis

## Single Step Grown NiFe Sponges as Efficient Water Splitting Electrocatalysts in Alkaline Medium

S. Thoufeeq, Dr. Pankaj Kumar Rastogi, Dr. Senoy Thomas, Anagandula Shravani, Dr. Tharangattu N. Narayanan, Prof. M. R. Anantharaman

Pages: 1385-1395 | First Published: 27 January 2020

A facile method is demonstrated to obtain nickel and iron based porous sponges, where by varying their precursor ratio, total water splitting



electrocatalysts can be developed. The NiFe based sponges are found to be efficient in water electrolysis and on par with some of the benchmarked catalysts so far reported.

[Abstract](#) | [Full text](#) | [PDF](#) | [References](#) | [Request permissions](#)

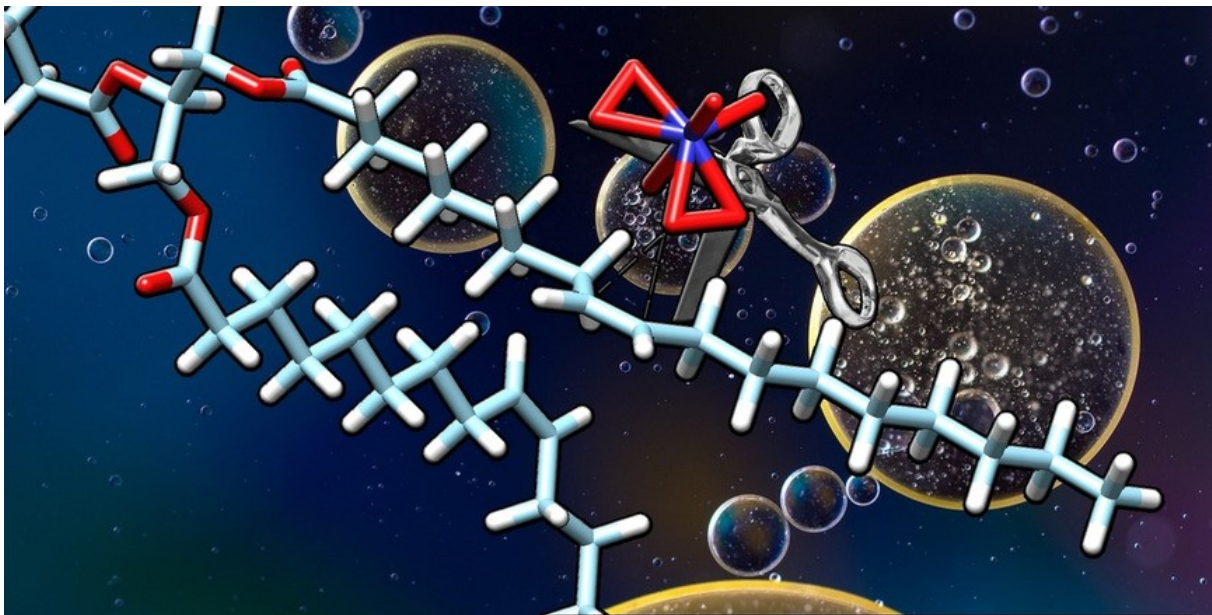
## Communications

### Sustainable Chemistry

#### Direct and Solvent-Free Oxidative Cleavage of Double Bonds in High-Oleic Vegetable Oils

Massimo Melchiorre, Dr. Vincenzo Benessere, Dr. Maria E. Cucciolito, Chiara Melchiorre, Prof. Francesco Ruffo, Dr. Roberto Esposito

Pages: 1396-1400 | First Published: 27 January 2020



High-oleic vegetable oils were oxidized with a catalytic system based on tungstic acid and hydrogen peroxide to produce azelaic glycerides. The process was applied also to a waste oil and resulted to be competitive with other double bond oxidative cleavage of simpler feedstocks.

[Abstract](#) | [Full text](#) | [PDF](#) | [References](#) | [Request permissions](#)

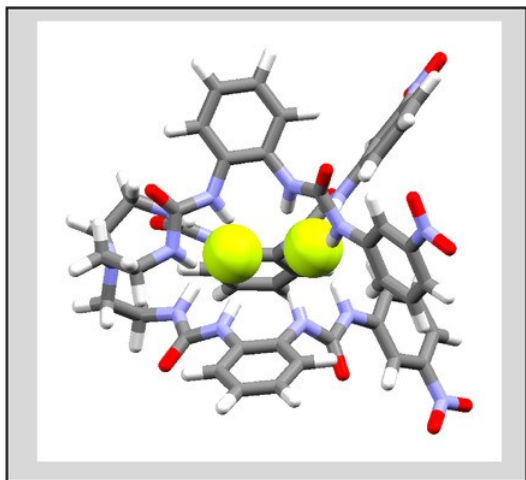
## Full Papers

## Organic &amp; Supramolecular Chemistry

## Cleft-Induced Ditung Binding of Spherical Halides with a Hexaurea Receptor

Bobby Portis, Dr. Ali Mirchi, Mohammad H. Hasan, Dr. Maryam Emami Khansari, Corey R. Johnson, Prof. Dr. Jerzy Leszczynski, Prof. Dr. Ritesh Tandon, Prof. Dr. Md. Alamgir Hossain

Pages: 1401-1409 | First Published: 27 January 2020



A tripodal-based hexaurea receptor with two clefts has been studied for spherical halides by  $^1\text{H}$  NMR, UV-Vis titrations, DFT calculations, demonstrating a ditopic binding for a halide with the binding strength in the order of fluoride > chloride > bromide > iodide. The strongest affinity for fluoride is due to the best adaptability of the two anions at the two clefts within the host's cavity.

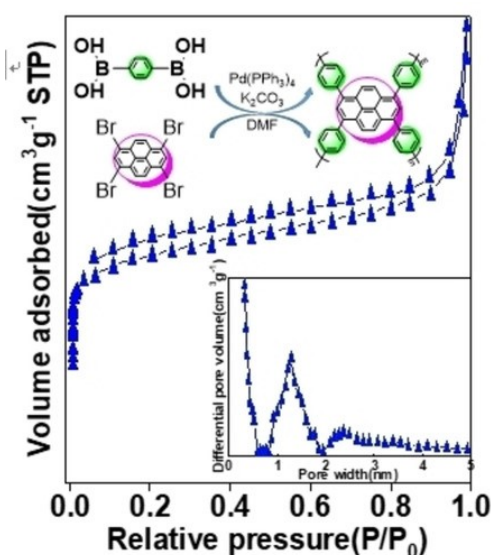
[Abstract](#) | [Full text](#) | [PDF](#) | [References](#) | [Request permissions](#)

## Materials Science inc. Nanomaterials &amp; Polymers

One-pot Facile Synthesis of Multifunctional Conjugated Microporous Polymers *via* Suzuki-Miyaura Coupling Reaction

Dao-Guang Teng, Prof. Xian-Yong Wei, Jia-Hao Li, Hua-Shuai Gao, Min Zhang, Prof. Zhi-Min Zong

Pages: 1410-1415 | First Published: 27 January 2020



Conjugated microporous polymer synthesized using 1,3,6,8-tetrabromopyrene and 1,4-phenylenediboronic acid exhibits the largest SSA up to  $1071\text{ m}^2\text{ g}^{-1}$ ,  $\text{H}_2$  uptake capacity of  $152.77\text{ cm}^3\text{ g}^{-1}$  (77 K, 1 bar) and  $\text{CO}_2$  uptake capacity of  $58.97\text{ cm}^3\text{ g}^{-1}$  (273 K, 1 bar). Moreover, the facile preparation strategy, outstanding thermal and fluorescent performances and high SSAs make CMPs promising candidates for the future industrial applications.

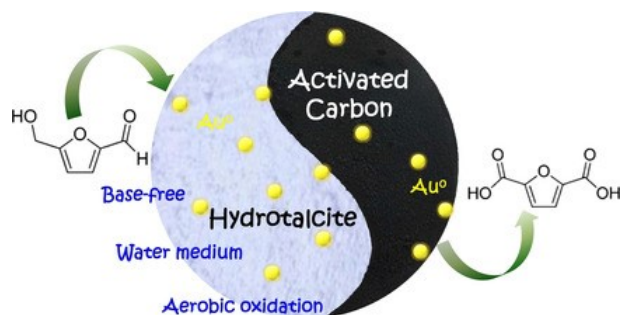
[Abstract](#) | [Full text](#) | [PDF](#) | [References](#) | [Request permissions](#)

## Catalysis

## Influence of Support Properties and Particle Size on the Gold-Catalyzed Base-Free Aerobic Oxidation of 5-Hydroxymethylfurfural

Weixiao Sun, Tianqi Gao, Guanghui Zhu, Prof. Qiue Cao, Dr. Wenhao Fang

Pages: 1416-1423 | First Published: 27 January 2020



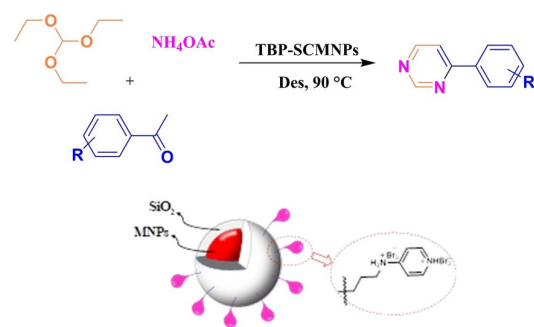
The structure-activity relationship of Au/HT-AC catalyst was studied for base-free aerobic oxidation of HMF to FDCA. The basic sites due to HT integrated with O-containing groups functionalized AC was favorable for adsorbing HMF and intermediates, promoting FDCA formation. The small Au NPs exposed a higher fraction of coordinatively unsaturated atoms were considered as the highly active sites for oxidizing hydroxyl and carbonyl groups

[Abstract](#) | [Full text](#) | [PDF](#) | [References](#) | [Request permissions](#)

### Synthesis of Pyrimidine Derivatives Catalyzed by Nanomagnetic Pyridinium-Tribromide Ionic Liquid

Azin Kharazmi, Prof. Ramin Ghorbani-Vaghei, Dr. Sedigheh Alavinia

Pages: 1424-1430 | First Published: 27 January 2020



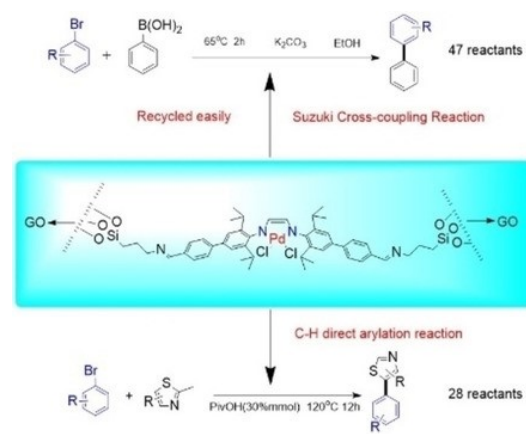
Multi-component reactions (MCRs) towards the synthesis of pyrimidine derivatives catalyzed was described using nano-magnetic pyridinium-tribromide (TBP-SCMNPs) as a novel efficient, recyclable and nanostructured catalyst in DES solvents at 90 °C.

[Abstract](#) | [Full text](#) | [PDF](#) | [References](#) | [Request permissions](#)

### Fabrication and Application of Graphene Supported Diimine-Palladium Complex Catalyst for Organic Synthesis

Yunlong Sun, Dr. Tian Li

Pages: 1431-1438 | First Published: 27 January 2020



The Pd-DI@GO can catalyze 47 reactants in Suzuki reaction, presenting extremely impressive yields of double and triple substitutions products (70~99%), only tiny Pd leaching (<1 ppm) was found in the reaction. The catalyst can be recycled easily after Suzuki reaction, exhibiting a yield above 90% for the 4th run. The Pd-DI@GO can also catalyze 28 reactants in C-H direct arylation reaction, affording 22 products with superior yields (>85%).

[Abstract](#) | [Full text](#) | [PDF](#) | [References](#) | [Request permissions](#)

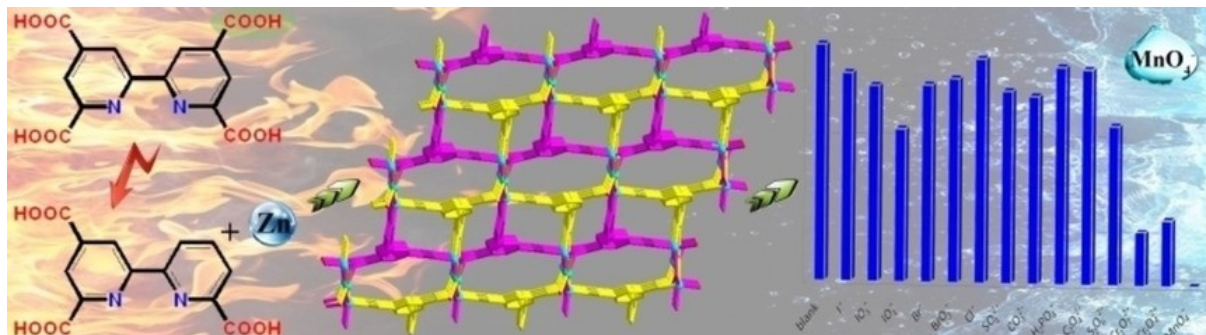


## Materials Science inc. Nanomaterials &amp; Polymers

## Synthesis, Structure and Fluorescent Property of a Novel 3D Rod-Packing Microporous Zn(II) MOF Based on a Temperature-Induced In Situ Ligand Reaction

Dr. Wen-Qian Zhang, Dr. Yi-Fan Kang, Dr. Lei-Lei Guo, Assist. Prof. Jun-Jie Yang

Pages: 1439-1442 | First Published: 27 January 2020



An in situ ligand reaction of decarboxylation has been happened during the self-assembly of a new MOF  $\{[Zn_{1.5}(\text{bptc}')(\text{H}_2\text{O})]\cdot\text{H}_2\text{O}\}_n$  (**1**) under a high-temperature hydrothermal condition, with  $\text{H}_4\text{bptc}$  ligand transforming into  $\text{H}_3\text{bptc}'$  ligand. MOF **1** reveals a rarely 3D double-walled rod-packing framework possessing three kinds of windows. In addition, MOF **1** shows high selectivity and sensitivity for  $\text{MnO}_4^-$  ion in aqueous solution by fluorescent quenching effect.

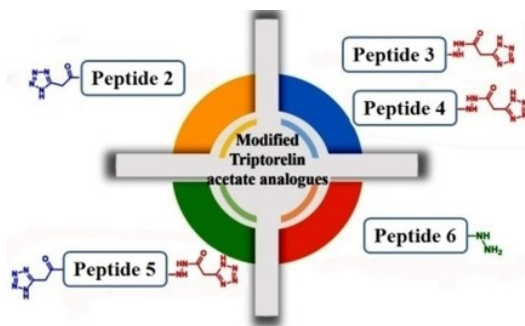
[Abstract](#) | [Full text](#) | [PDF](#) | [References](#) | [Request permissions](#)

## Organic &amp; Supramolecular Chemistry

## Design, Synthesis and Biological Evaluation of Triptorelin Analogs Containing Tetrazole Moiety

Hamidreza Sohbaty, Dr. Mohsen Alipour, Prof. Saman Hosseinkhani, Prof. Saeed Balalaie, Dr. Fatima Hamdan

Pages: 1443-1449 | First Published: 27 January 2020



An efficient approach for the synthesis of triptorelin acetate analogues is described. To achieve this goal tetrazole moiety as bioisostere of carboxylic acid was added in the C- or N-terminus of the synthetic peptides. The synthesis of target peptides was done based on solid phase peptide synthesis approach. The biological activity of the synthesized peptides was investigated and compared to the triptorelin acetate.

[Abstract](#) | [Full text](#) | [PDF](#) | [References](#) | [Request permissions](#)

## Materials Science inc. Nanomaterials &amp; Polymers

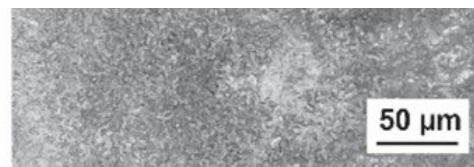
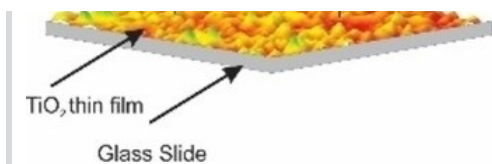
A Facile Preparation of Transparent Ultrahydrophobic Glass via  $\text{TiO}_2$ /Octadecyltrichlorosilane (ODTS) Coatings for Self-Cleaning Material

Nurul Pratiwi, Dr. Zulhadjri, Prof. Dr. Syukri Arief, Dr. Diana Vanda Wellia

Pages: 1450-1454 | First Published: 27 January 2020







Transparent ultrahydrophobic glass was successfully fabricated by depositing the  $\text{TiO}_2$  thin film and octadecyltrichlorosilane (ODTS) through a simple, facile and environmentally friendly method. The modified glass showed high water contact angle of  $146^\circ$  and excellent self-cleaning properties, which could easily roll-off the dirt particles from the glass surface with the help of water droplets.

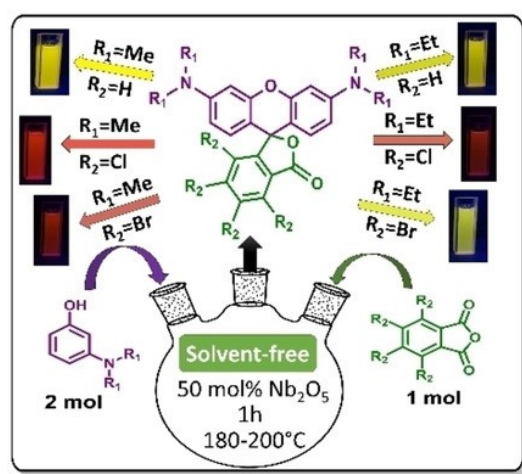
[Abstract](#) | [Full text](#) | [PDF](#) | [References](#) | [Request permissions](#)

## Organic & Supramolecular Chemistry

### Solvent-Free Synthesis Using $\text{Nb}_2\text{O}_5$ and a Theoretical-Experimental Study of Solvent Effect in New Rhodamine Dyes

Dr. Bruno Henrique Sacoman Torquato da Silva, Luiza Olbera Riehl, Dr. Giovanni Carvalho dos Santos, Juan Carlos Roldao, Dr. Luiz Carlos da Silva-Filho

Pages: 1455-1463 | First Published: 27 January 2020



In this paper is described the solvent-free synthesis of rhodamine derivatives using  $\text{Nb}_2\text{O}_5$  as catalyst, obtaining these promising dyes in high yields in just one hour of reaction time, with catalyst recovery. The synthesized rhodamines showed great photophysical properties, with absorption and emission bands in the visible region and a high quantum yield. It is also reported a theoretical-experimental study of solvent effect on the structures of these molecules.

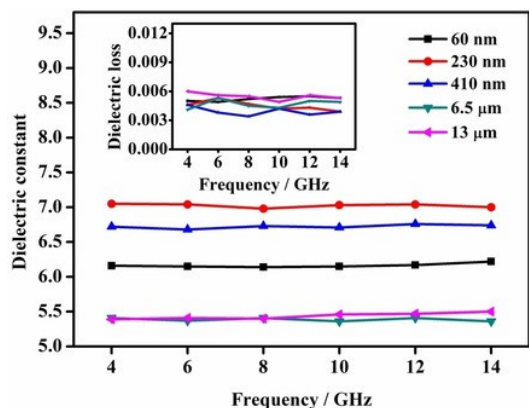
[Abstract](#) | [Full text](#) | [PDF](#) | [References](#) | [Request permissions](#)

## Materials Science inc. Nanomaterials & Polymers

## The Effects of Concentration and Particle Size of TiO<sub>2</sub> on the Dielectric Properties of Polyolefin-Based Microwave Substrates

Chunyan Wang, Dr. Bo Wu, Dr. Xin Mao, Ting Deng, Rong Li, Yi Xu, Prof. Xianzhong Tang

Pages: 1464-1469 | First Published: 27 January 2020



Fibre-reinforced PB/SBS/EPDM/TiO<sub>2</sub> copper clad substrates were prepared. Results indicated that the substrate with 230 nm TiO<sub>2</sub> at 70 wt% loading exhibited high permittivity (7.03) and low dielectric loss (0.0042) at 10 GHz.

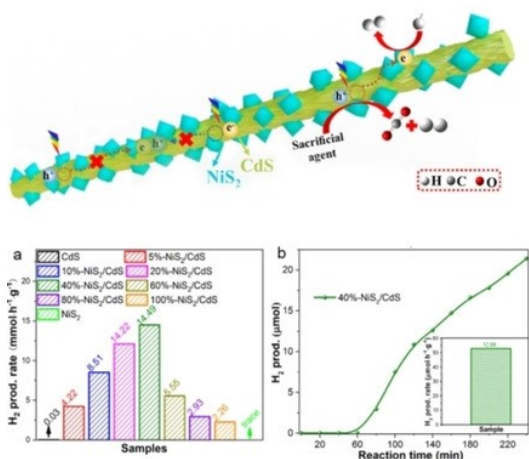
[Abstract](#) | [Full text](#) | [PDF](#) | [References](#) | [Request permissions](#)

## Energy Technology & Environmental Science

### Cellulose as Sacrificial Biomass for Photocatalytic Hydrogen Evolution over One-dimensional CdS Loaded with NiS<sub>2</sub> as a Cocatalyst

Dr. Chunhe Li, Dr. Sara Bonabi Naghadeh, Dr. Liping Guo, Ke Xu, Prof. Jin Zhong Zhang, Prof. Hongmei Wang

Pages: 1470-1477 | First Published: 27 January 2020



NiS<sub>2</sub>/CdS nanocomposites with varying amount of NiS<sub>2</sub> were synthesized via a two-step approach and characterized for sustainable hydrogen evolution. The optimal 40%-NiS<sub>2</sub>/CdS nanocomposite exhibited H<sub>2</sub> evolution rate of 14.49 mmol·h<sup>-1</sup>·g<sup>-1</sup> in lactic acid aqueous solution, much higher than that of pure CdS. In addition, the 40%-NiS<sub>2</sub>/CdS nanocomposite showed a H<sub>2</sub> evolution rate of 52.88 μmol·h<sup>-1</sup>·g<sup>-1</sup> with only cellulose as sacrificial agent. This study shows the good potential of NiS<sub>2</sub>/CdS nanocomposites for photocatalytic hydrogen evolution utilizing cellulosic biomass.

[Abstract](#) | [Full text](#) | [PDF](#) | [References](#) | [Request permissions](#)

## Reviews

### Materials Science inc. Nanomaterials & Polymers

#### Solubility and Bioavailability of Fenofibrate Nanoformulations

Dr. Raj Kumar

Pages: 1478-1490 | First Published: 27 January 2020





Fenofibrate is a hypolipidemic drug with poor water solubility. This review focus on the enhancement of solubility and bioavailability of fenofibrate through several nanotechnology-based approaches i. e. milling, antisolvent precipitation, sonochemistry, supercritical fluids, spray drying, self-emulsifying drug delivery system, solid lipid nanoparticles, and silica based nanoformulations including literature reports have been explored.

[Abstract](#) | [Full text](#) | [PDF](#) | [References](#) | [Request permissions](#)

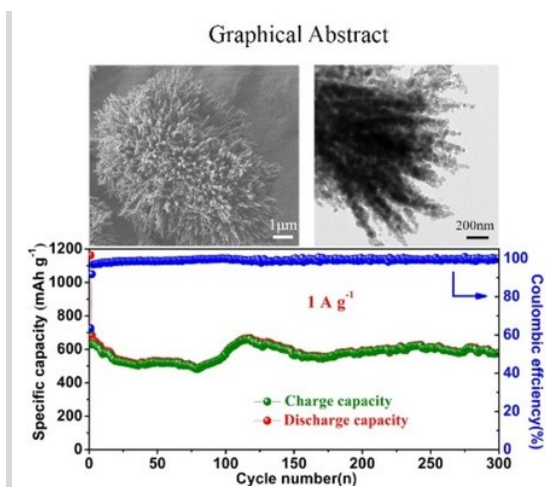
## Full Papers

### Materials Science inc. Nanomaterials & Polymers

#### A Facile Synthesis of Urchin-Like $\text{ZnMn}_2\text{O}_4$ Architectures with Enhanced Electrochemical Lithium Storage

Dr. Xiaoyong Dou, Dr. Ming Chen, Prof. Jiantao Zai, Dr. Yong Gong, Dr. Asma Iqbal, Qinnan Zhou, Boxu Dong, Dr. TsegayeTadesse Tsega, Prof. Rongrong Qi, Prof. Xuefeng Qian

Pages: 1491-1495 | First Published: 27 January 2020



This work reported a facile synthetic methodology for  $\text{ZnMn}_2\text{O}_4$  hierarchical architectures with urchin-like structure. As anode materials for Lithium-ion batteries, the as-prepared  $\text{ZnMn}_2\text{O}_4$  electrodes showed high reversible capacity (889 mAh g<sup>-1</sup> after 150 cycles at current density of 0.4 A g<sup>-1</sup>), excellent rate capability, and long cycling (578 mAh g<sup>-1</sup> after 300 cycles at current density of 1 A g<sup>-1</sup>). The urchin-like  $\text{ZnMn}_2\text{O}_4$  architectures would be a promising anode with high performances for Lithium-ion batteries.

[Abstract](#) | [Full text](#) | [PDF](#) | [References](#) | [Request permissions](#)

### Energy Technology & Environmental Science

#### Different Enhancement Mechanisms of the Anodizing Al-Doped or Sn-Coupled $\text{Ti}_3\text{SiC}_2$ for the Photoelectrochemical Performance

Prof. Hongfeng Yin, Dr. Zhiwei Wang, Prof. Yun Tang, Dr. Muralidhar Chourashiya, Dr. Xiuting Li, Dr. Hudie Yuan, Nan Yan, Prof. Xiaohu Ren

Pages: 1496-1505 | First Published: 30 January 2020

Among anodized Al or Sn introduced  $\text{Ti}_3\text{SiC}_2$  (Al-ATSC or Sn-ATSC) samples, superior photocurrents of Al<sub>0.5</sub>-ATSC and Sn<sub>0.1</sub>-ATSC under visible light irradiation are respectively 18 and 16 times higher than anodized  $\text{Ti}_3\text{SiC}_2$ , which are realized by the different strategies of doping Al or coupling  $\text{SnO}_2$  on the basis of the  $\text{TiO}_2$ .

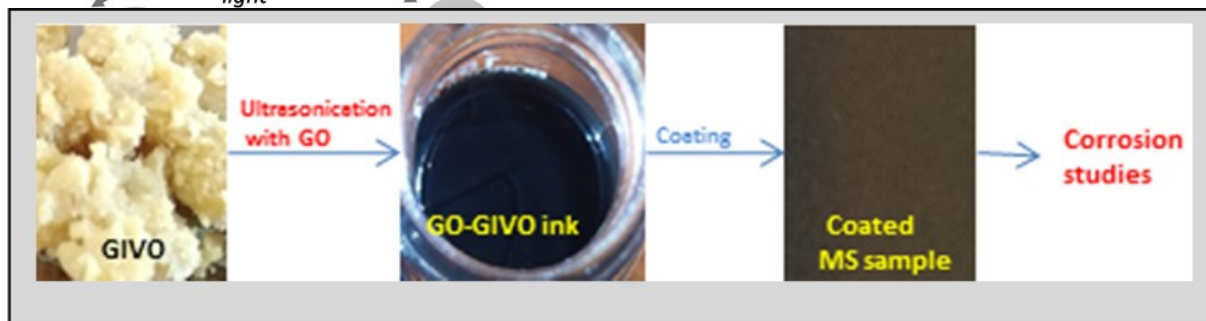
[Abstract](#) | [Full text](#) | [PDF](#) | [References](#) | [Request permissions](#)

### Materials Science inc. Nanomaterials & Polymers

#### A Sustainable and Eco-Friendly Polymer Based Graphene Oxide Nanocomposite Anti-Corrosion Coating on Mild Steel

Mahesh B. Hegde, Prof. Kikkeri N. Mohana

Pages: 1506-1515 | First Published: 30 January 2020



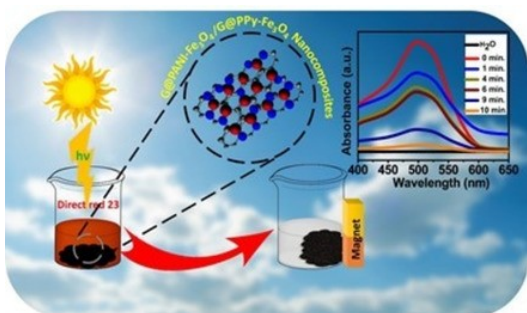
The graphene oxide incorporated *Garcinia indica* vegetable oil based anticorrosion coating on mild steel specimen is fabricated through thermal polymerization of graphene oxide-*Garcinia indica* vegetable oil dispersion. The electrochemical impedance and Tafel polarization studies of coated mild steel sample exhibited excellent corrosion protection behaviour with 99.9 % corrosion prevention efficiency. The composite coating showed very good stability even after one year of exposure in open atmosphere.

[Abstract](#) | [Full text](#) | [PDF](#) | [References](#) | [Request permissions](#)

### One-Pot Synthetic Approach for Magnetically Separable Graphene Nanocomposite for Dye Degradation

Dattatray A. Pethsangave, Rahul V. Khose, Pravin H. Wadekar, Dnyaneshwar K. Kulal, Dr. Surajit Some

Pages: 1516-1525 | First Published: 30 January 2020



In this work, we have developed a one-pot, simple and eco-friendly process for the synthesis of magnetically separable graphene nanocomposites, which are effective for degradation of dye pollutant.

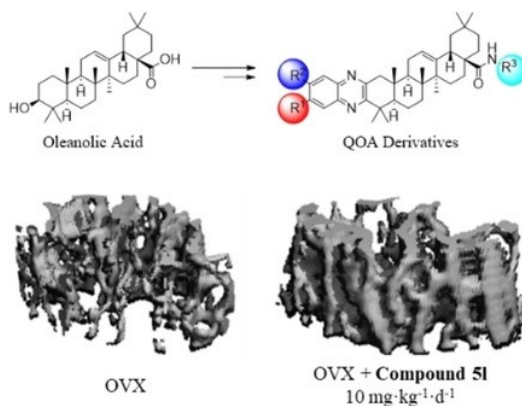
[Abstract](#) | [Full text](#) | [PDF](#) | [References](#) | [Request permissions](#)

## Medicinal Chemistry & Drug Discovery

### Modified Quinoxaline-Fused Oleanolic Acid Derivatives as Inhibitors of Osteoclastogenesis and Potential Agent in Anti-Osteoporosis

Yu-Chao Zhang, Dr. Qi Shen, Ming-Wu Zhu, Jie Wang, Yun Du, Dr. Jing Wu, Prof. Jian-Xin Li

Pages: 1526-1533 | First Published: 30 January 2020



Series of novel quinoxaline-fused oleanolic acid (QOA) derivatives were synthesized. These compounds significantly inhibited RANKL-induced formation of osteoclasts. QOA derivatives **51** ( $IC_{50}=62.4\text{ nM}$ ) exhibited quite a potent activity. Compound **51** could attenuate bone loss in the bilateral ovariectomy (OVX) mice model.

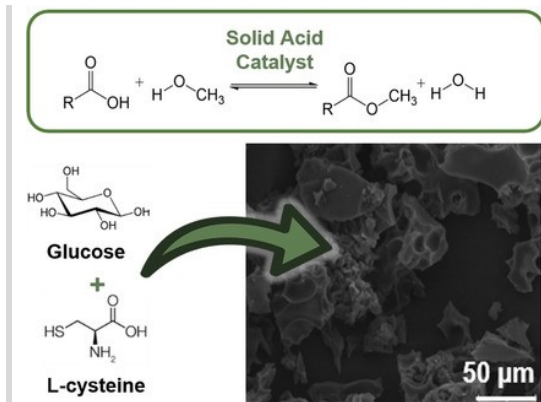
[Abstract](#) | [Full text](#) | [PDF](#) | [References](#) | [Request permissions](#)

## Sustainable Chemistry

### Biofuel Production With Sulfonated High Surface Area Carbons Derived From Glucose

Dr. Shiba P. Adhikari, Dr. Zachary D. Hood, Sara Borchers, Dr. Marcus Wright, Prof. Abdou Lachgar

Pages: 1534-1538 | First Published: 30 January 2020



"Sweet" solid acid catalysts: We report the first demonstration of a sugar-derived, L-cysteine-modified, high surface area carbon as effective catalysts for converting free fatty acids, those commonly found in waste cooking oil, to biofuels. This development is expected to impact the production of biofuels on the basis of catalyst separation and choice of feedstock.

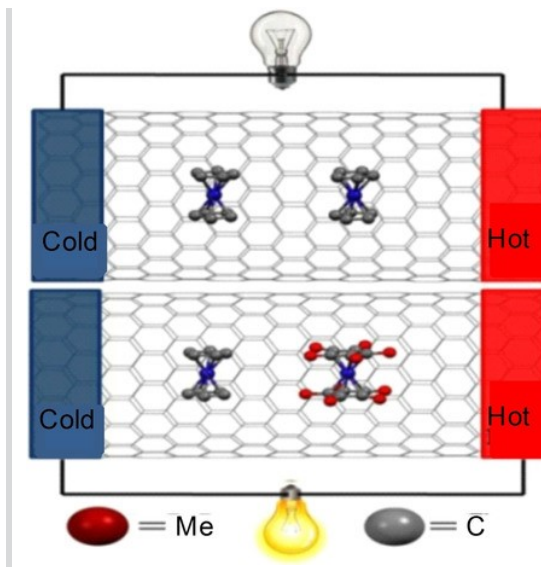
[Abstract](#) | [Full text](#) | [PDF](#) | [References](#) | [Request permissions](#)

## Electro, Physical & Theoretical Chemistry

### A Novel Way to Enhance the Thermoelectric Efficiency of Carbon Nanotube through Cobaltocene-decamethyl Cobaltocene Encapsulation

Sayantanu Koley, Dr. Sabyasachi Sen, Dr. Swapan Chakrabarti

Pages: 1539-1546 | First Published: 30 January 2020



Symmetry Breaking Can Improve the Thermoelectric Ability of Carbon Nanotube  
Experimental findings show that thermoelectric figure of merit of carbon nanotube can be increased six times by encapsulating cobaltocene inside it. Our in-silico findings illustrate that a  $10^3$  times increase is possible by simultaneous encapsulation of cobaltocene and decamethyl cobaltocene instead of cobaltocene. Such an encapsulation improves the electrical conductance of the material by breaking the symmetry of the molecule. Consequently the thermoelectric figure of merit of the material enhances.

[Abstract](#) | [Full text](#) | [PDF](#) | [References](#) | [Request permissions](#)

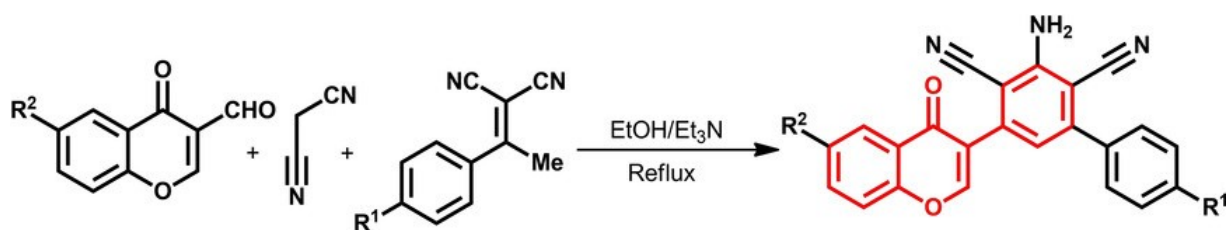
## Organic & Supramolecular Chemistry

### A Catalyst-Free Synthetic Route to Modified Isoflavone *via* Multi-Component Reaction

Prof. Abdolali Alizadeh, Akram Bagherinejad



Pages: 1547-1551 | First Published: 30 January 2020



A series of modified isoflavones have been synthesized in excellent yields (60–85 %) *via* a one-pot three-component reaction of 3-formylchromones, malononitrile, various  $\alpha,\alpha$ -dicyanoolefins, using  $\text{Et}_3\text{N}$  as the base, and EtOH as the solvent, in good yield. The value of this method lies in its short reaction time, convenient purification, no need for a metal catalyst, good efficiency, and green solvent. This synthesis involves a Knoevenagel condensation/carbanion formation/ring closure, and finally an elimination to obtain the respective isoflavonoid derivatives.

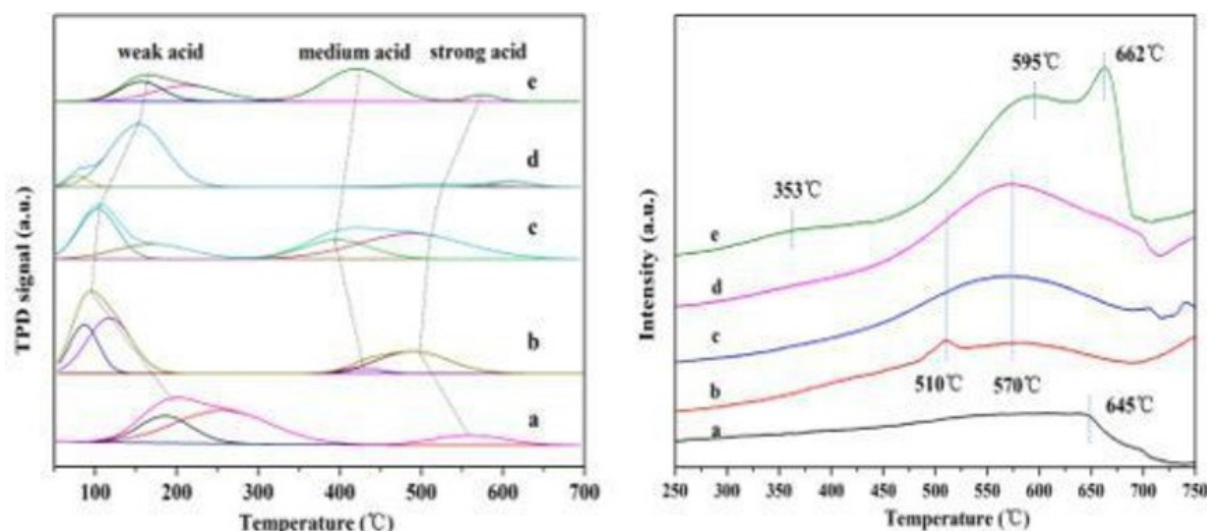
[Abstract](#) | [Full text](#) | [PDF](#) | [References](#) | [Request permissions](#)

## Catalysis

### Amorphous Porous Chromium-Zirconium Bimetallic Phosphate: Synthesis, Characterization and Application in Liquid Phase Oxidation of Hydrocarbons by Different Oxygen Sources

Lei Sun, Deyu Kong, Prof. Fang Wang, Wei Luo, Yanqiu Chen, Zhouzhou, Prof. Junhua Liu

Pages: 1552-1559 | First Published: 30 January 2020



The Cr–Zr bimetallic phosphate catalysts with different Cr/Zr molar ratio were prepared by sol-gel method, two types of active sites - acidic and redox sites are found in these catalysts. The acidic and redox sites on catalyst surface are affected by the different addition of chromium ions, and formation of mesoporous structure leads to the uniform dispersion of acidic and redox sites. These two active centers in the bimetallic phosphates play the synergistic catalytic role in the oxidation of C–H bond.

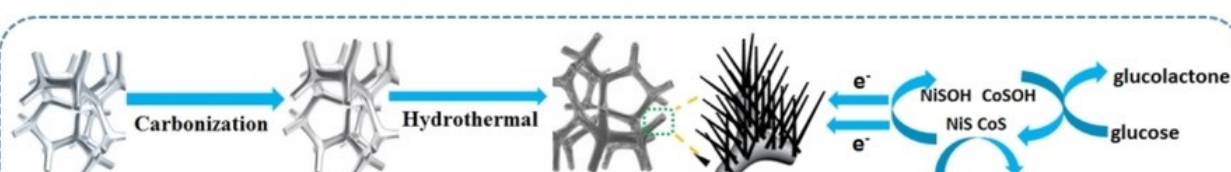
[Abstract](#) | [Full text](#) | [PDF](#) | [References](#) | [Request permissions](#)

## Analytical Chemistry

### NiCo<sub>2</sub>S<sub>4</sub> Nanowire-Decorated Flexible Carbon Foam for Sensitive Glucose Sensors

Yi He, Tingting Wu, Shihan Tao, Lijuan Liu, Jun Wu, Prof. Qiaohui Guo

Pages: 1560-1566 | First Published: 30 January 2020



3DMF

3DCF

 $\text{NiCo}_2\text{S}_4/3\text{DCF}$  $\text{OH}^-$  $\text{H}_2\text{O}$ 

$\text{NiCo}_2\text{S}_4$  nanostructures have attracted much attention in electrochemistry due to its highly catalytic activity and low cost.  $\text{NiCo}_2\text{S}_4$  arrays grown on 3D carbon foam ( $\text{NiCo}_2\text{S}_4/3\text{DCF}$ ) is presented by a two-pot hydrothermal method, and further applied for glucose sensor.  $\text{NiCo}_2\text{S}_4/3\text{DCF}$  shows a self-standing structure and was used as electrode directly. This sensor displays a wide linear range (0.005–13.07 mM), low detection limit and good selectivity.

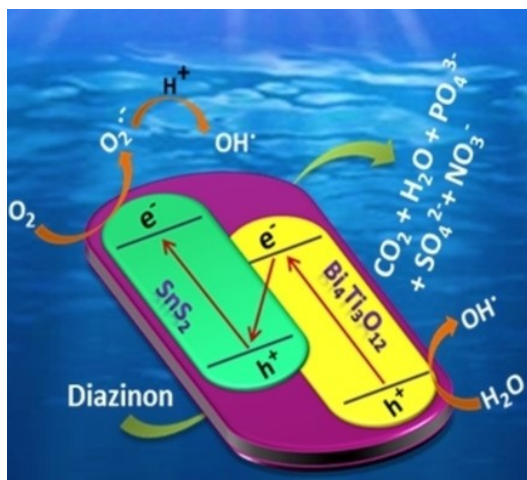
[Abstract](#) | [Full text](#) | [PDF](#) | [References](#) | [Request permissions](#)

## Catalysis

### $\text{SnS}_2/\text{Bi}_4\text{Ti}_3\text{O}_{12}$ Heterostructure Material: A UV-Visible Light Active Direct Z-Scheme Photocatalyst for Aqueous Phase Degradation of Diazinon

Krishnendu Das, Dibyananda Majhi, Ranjit Bariki, Dr. Braja G. Mishra

Pages: 1567-1577 | First Published: 30 January 2020



A sustainable photocatalytic degradation route is developed for mineralization of diazinon insecticide from aqueous sources using  $\text{SnS}_2/\text{Bi}_4\text{Ti}_3\text{O}_{12}$  heterostructure materials as photocatalyst under visible light irradiation. The photocatalyst operates through a direct Z-scheme electron transfer mechanism to generate highly reactive  $\cdot\text{OH}$  and  $\text{O}_2\cdot^-$  radicals responsible for diazinon photodegradation.

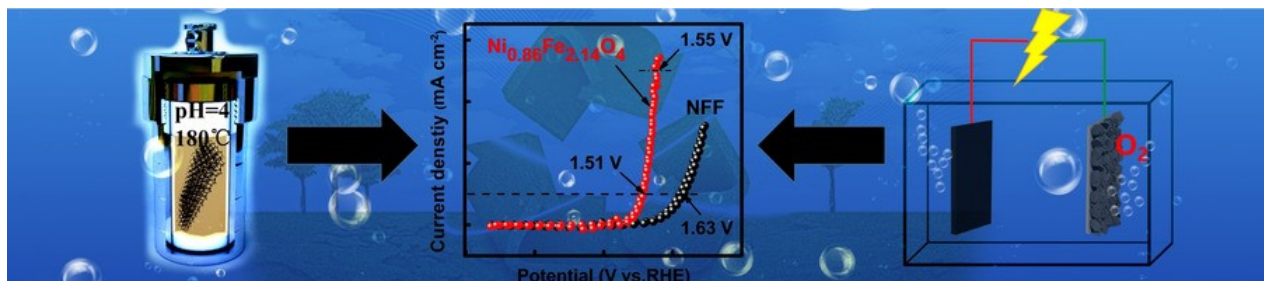
[Abstract](#) | [Full text](#) | [PDF](#) | [References](#) | [Request permissions](#)

## Sustainable Chemistry

### Alloy Foam-Derived $\text{Ni}_{0.86}\text{Fe}_{2.14}\text{O}_4$ Hexagonal Plates as an Efficient Electrochemical Catalyst for the Oxygen Evolution Reaction

Xiaoxing Kong, Jinlong Lei, Qinghe Cao, Dr. Fenggang Liu, Chuqi Xie, Miao Huang, Dr. Xingdong Xu, Prof. Jiahai Wang

Pages: 1578-1585 | First Published: 30 January 2020



The seamless growth of a three-dimensional (3D) intertwined  $\text{Ni}_{0.86}\text{Fe}_{2.14}\text{O}_4$  hexagonal plate directly from a Ni–Fe alloy foam substrate is successfully designed and prepared. The  $\text{Ni}_{0.86}\text{Fe}_{2.14}\text{O}_4$  exhibited excellent electrochemical properties and prominent electrochemical durability for the oxygen evolution reaction. The synergistic effect between Ni and Fe in  $\text{Ni}_{0.86}\text{Fe}_{2.14}\text{O}_4$  and the seamless connection between  $\text{Ni}_{0.86}\text{Fe}_{2.14}\text{O}_4$  and the substrate make main contribution to excellent OER activity for the electrode system.

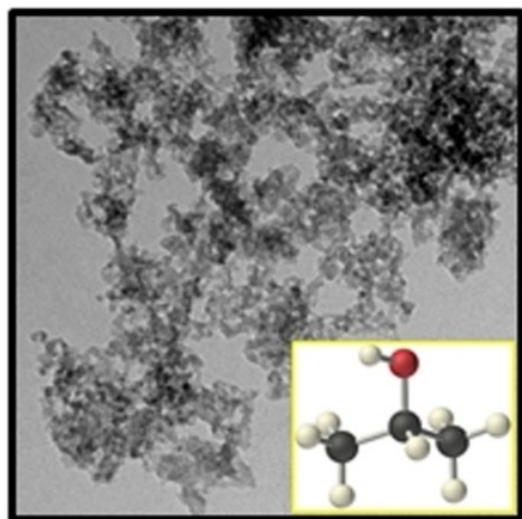
[Abstract](#) | [Full text](#) | [PDF](#) | [References](#) | [Request permissions](#)

## Inorganic Chemistry

## Effect of Aging Solvents on Physicochemical and Thermal Properties of Silica Xerogels Derived from Steel Slag

Gulcihan Guzel Kaya, Prof. Huseyin Deveci

Pages: 1586-1591 | First Published: 30 January 2020



Silica xerogel was synthesized from steel slag by sol-gel process under ambient pressure drying. Isopropanol as an aging solvent had synergistic effects on the physicochemical and thermal properties of silica xerogel. Highly porous structure of silica xerogel aged in isopropanol provided lower density and thermal conductivity.

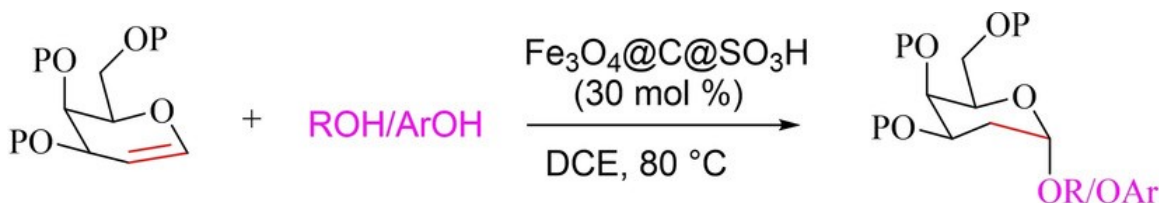
[Abstract](#) | [Full text](#) | [PDF](#) | [References](#) | [Request permissions](#)

## Sustainable Chemistry

Core-Shell  $\text{Fe}_3\text{O}_4@\text{Carbon}@\text{SO}_3\text{H}$ : A Powerful Recyclable Catalyst for the Synthesis of  $\alpha$ -2-Deoxygalactosides

Nan Jiang, Youxian Dong, Guosheng Sun, Guofang Yang, Qingbing Wang, Prof. Jianbo Zhang

Pages: 1592-1596 | First Published: 30 January 2020



P=Ac, Et, Bn, Allyl, TBS

A method for the preparation of 2-deoxygalactosides by using a novel magnetic core-shell material  $\text{Fe}_3\text{O}_4@\text{C}@\text{SO}_3\text{H}$  as a catalyst was developed. The method had the advantages of short reaction time (1–4 h), good to excellent yield (69–93 %), high stereoselectivity ( $\alpha:\beta > 30:1$ ), one-pot synthesis of trisaccharides. Moreover, the catalyst retained good catalytic activity after five times recycling, and the yield did not change significantly.

[Abstract](#) | [Full text](#) | [PDF](#) | [References](#) | [Request permissions](#)

## Energy Technology &amp; Environmental Science

## A Hybrid Electrochemical Energy Storage Device Using Sustainable Electrode Materials

Dr. Manickam Minakshi, Dr. David R. G. Mitchell, Dr. Robert T. Jones, Dr. Nimai Chand Pramanik, Dr. Annelise Jean-Fulcrand, Prof. Georg Garnweitner

Pages: 1597-1606 | First Published: 30 January 2020

Electrochemical energy storage device, comprising a faradaic rechargeable pseudo-capacitor type electrode with a non-faradaic rechargeable capacitor electrode, is successfully developed. In this work, we present a new approach to design electrodes, fabricated from sustainable resources by hybridizing calcined eggshell capacitor anode with a mixed binary metal oxide pseudo-capacitor cathode.

Abstract | Full text | PDF | References | Request permissions

Submit a Manuscript | Discharge | Browse free sample issue | OH<sup>-</sup> | Charge | Get content alerts | Subscribe to this journal

More from this journal

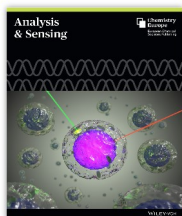
Reviews  
Editorials  
Video Abstracts

**One App**  
18 chemical society journals

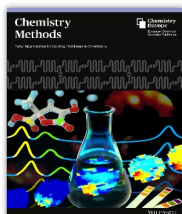
Angewandte Chemie  
ACES  
Chemistry Europe

Download on the App Store  
GET IT ON Google Play

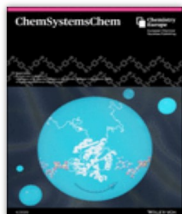
**Chemistry Europe**  
European Chemical Societies Publishing



**NEW JOURNAL:**  
[Analysis & Sensing](#)  
Accepting submissions now.



**NEW JOURNAL:**  
[Chemistry—Methods](#)  
Accepting submissions now.



**ISSUE**  
Volume 2, Issue 4  
July 2020



ISSUE

Volume 26, Issue 43

Pages: 9403-9651

August 3, 2020

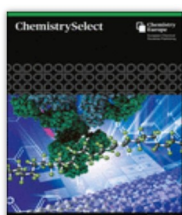


ISSUE

Volume 9, Issue 8

Pages: 793-817

August 2020

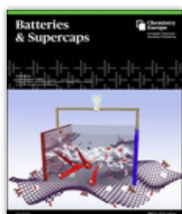


ISSUE

Volume 5, Issue 29

Pages: 8881

August 7, 2020

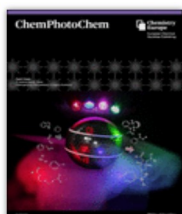


ISSUE

Volume 3, Issue 7

Pages: 566-667

July 2020

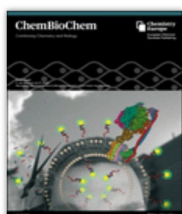


ISSUE

Volume 4, Issue 7

Pages: 451-534

July 2020



ISSUE

Volume 21, Issue 15

Pages: 2086-2224

August 3, 2020



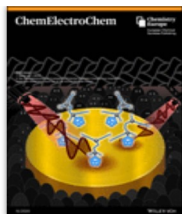
ISSUE

Volume 12, Issue 14

Pages: 3598-3792

July 21, 2020



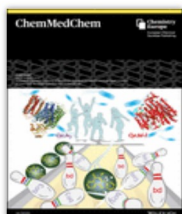


ISSUE

Volume 7, Issue 15

Pages: 3168-3310

August 3, 2020

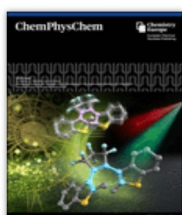


ISSUE

Volume 15, Issue 14

Pages: 1243-1371

July 20, 2020

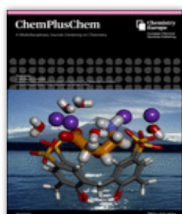


ISSUE

Volume 21, Issue 14

Pages: 1483-1616

July 17, 2020



ISSUE

Volume 85, Issue 8

Pages: 1612-1638

August 2020



ISSUE

Volume 13, Issue 14

Pages: 3539-3725

July 22, 2020



ISSUE

Volume 2020, Issue 29

Pages: 2767-2849

August 9, 2020



ISSUE

Volume 2020, Issue 29

Pages: 4433-4638

August 9, 2020



ChemistryViews.org Home

## Your Chemistry Hero

03 Aug 2020

Who do you admire in chemistry? What makes a hero for you? – anniversary contest for August

## Nanoparticle Catalyst with All Six Platinum-Group Metals

03 Aug 2020

High-entropy-alloy nanoparticles can catalyze complex reactions

## Smelling Molecular Conformations

03 Aug 2020

Olfactory receptor recognizes different conformationally restricted octanal analogues

## Chemistry Europe Virtual Events

02 Aug 2020

Virtual symposia and talks organized by the editorial offices and board members of Chemistry Europe journals

## Electronics Waste Reused as Protective Coating

02 Aug 2020

Old printed circuit boards and computer monitors converted to strong coating for steel

**ACES** Asian Chemical  
Editorial Society



ISSUE

Volume 15, Issue 15

The Chemistry of 2D Materials Membranes

Pages: 2239-2378

August 3, 2020



ISSUE

Volume 9, Issue 7

Pages: 967-1086

July 2020



ISSUE

Volume 6, Issue 7

Pages: 996-1135

July 2020

© 2020 WILEY-VCH Verlag GmbH & Co. KGaA, Weinheim

About Wiley Online Library

**Privacy Policy**

**Terms of Use**

**Cookies**

**Accessibility**

Help & Support

**Contact Us**

Opportunities

**Subscription Agents**

**Advertisers & Corporate Partners**

Connect with Wiley

**The Wiley Network**

**Wiley Press Room**

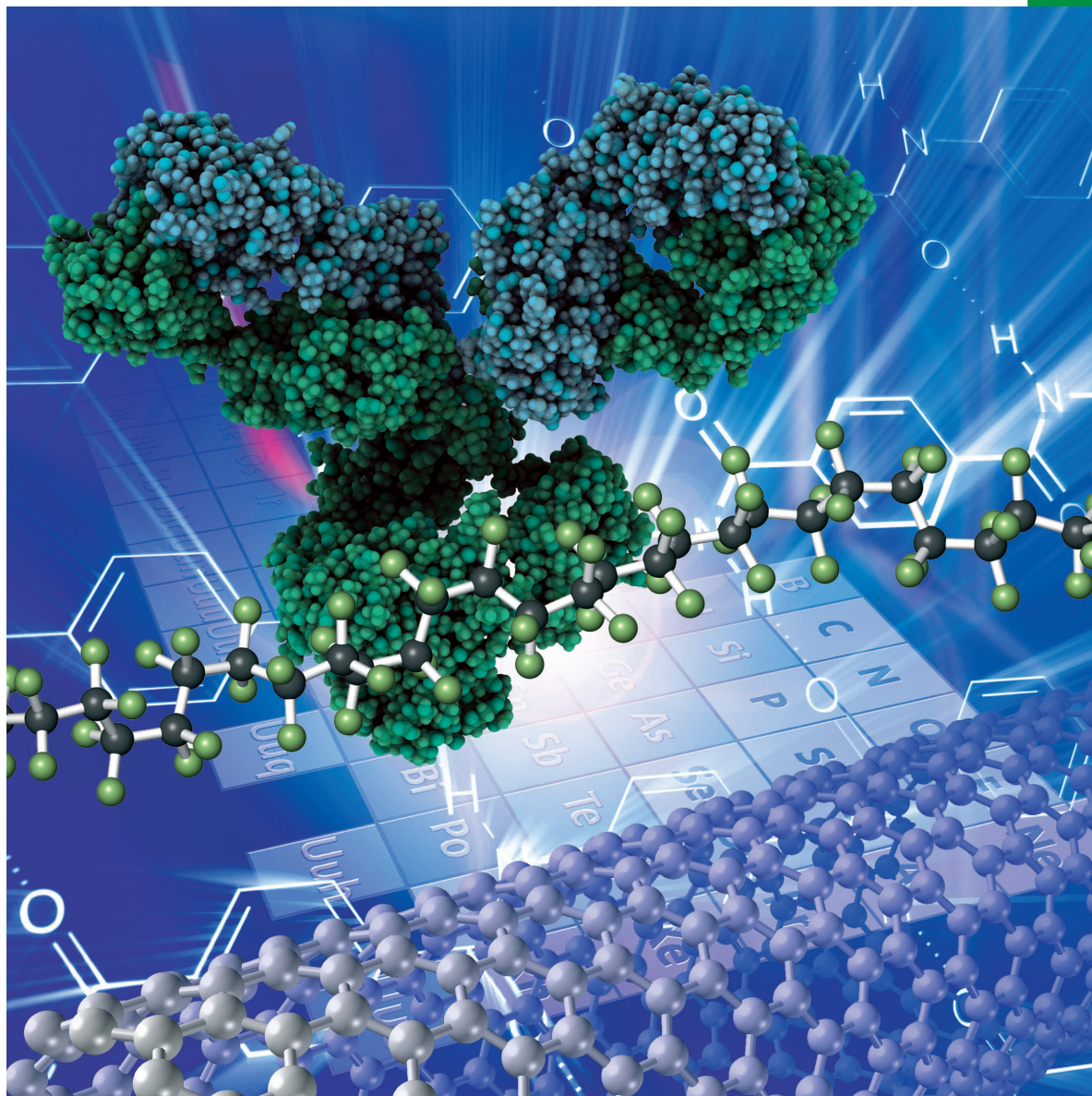
Copyright © 1999-2020 John Wiley & Sons, Inc. All rights reserved

# Chemistry *SELECT*



[www.chemistryselect.org](http://www.chemistryselect.org)

A journal of



## REPRINT

WILEY-VCH



Materials Science inc. Nanomaterials &amp; Polymers

# A Facile Preparation of Transparent Ultrahydrophobic Glass via TiO<sub>2</sub>/Octadecyltrichlorosilane (ODTS) Coatings for Self-Cleaning Material

Nurul Pratiwi, Zulhadjri, Syukri Arief, and Diana Vanda Wellia<sup>\*[a]</sup>

A facile strategy was developed to fabricate transparent ultrahydrophobic glass. First, TiO<sub>2</sub> films were deposited uniformly on untreated glass substrate after heating aqueous peroxotitanate thin films at 120 °C for 1 h followed by octadecyltrichlorosilane (ODTS) modification. The as-fabricated surfaces were then possessed ultrahydrophobic properties because of the combination of the rough surface topography of TiO<sub>2</sub> and low surface energy due to ODTS monolayer. It was found that the

water contact angle and sliding angle of the as-prepared coatings were about 146° and 7°, respectively. Besides, these coatings showed excellent self-cleaning performance compared to untreated glass in order to remove dirt particles with water droplets. It is believed that the current method could lead as low-cost and effective way to fabricate a very promising material for commercial and industrial coatings applications.

## 1. Introduction

Glass is one of the most important materials that widely used for the exterior of high buildings, car window and solar glass.<sup>[1]</sup> However in a natural environment, the accumulation of dust particles or other contaminants on glass surface causes a serious problem, which requires high maintenance cost to make it clean.<sup>[2]</sup> Recently, self-cleaning coating based on hydrophobicity on the glass surface is proposed as one of the possible solutions to maintain the durability of this material against dust accumulation.<sup>[3–5]</sup> The requirements for this type of coating have adopted from distinctive structural and functional properties of lotus leaves.<sup>[6]</sup> It has been found that the self-cleaning property of lotus is mainly due to its structured roughness surface in combination with the low surface energy of biological epicuticular wax crystals.<sup>[7]</sup> Hence, lotus leaf has a static contact angle  $\geq 150^\circ$  and sliding angle  $< 10^\circ$ , then this such a surface known as superhydrophobic.<sup>[8,9]</sup> The term of ultrahydrophobic, alternatively, has been used to describe a surface that exhibits between advancing and receding contact angles of  $150^\circ$ .<sup>[10]</sup> Therefore, rough surface topography and low surface energy are two typical factors that require in realizing the water repellent or hydrophobicity of solid surfaces.<sup>[11]</sup>

Up to now, various methods have been developed to prepare artificial highly hydrophobic coatings. However, most of these techniques involve high cost and complexity procedures.<sup>[12]</sup> But, the wet-chemical methods such as sol-gel method combining with dip or spin coating technique are well known and more flexible in approach to form a cost-efficient

hydrophobic coatings. For instance, Wang et al.<sup>[12]</sup> developed sol-gel methods to fabricate hydrophobic coating using TiO<sub>2</sub> and stearic acid. The prepared coating exhibited semi-transparent and thermal-stable hydrophobic surface with static water contact angle (WCA) as high as  $157^\circ$ . Syafiq et al.<sup>[13]</sup> proposed a simple and low-cost sol-gel system in which TiO<sub>2</sub> inorganic nanoparticles were incorporated in isooctyltrimethoxysilane (ITMS) to fabricate hydrophobic coatings. As a result, an opaque superhydrophobic nano-TiO<sub>2</sub>/ITMS possess excellent self-cleaning performances against dilute ketchup solution, mud and silicon powder compared to single-phase ITMS coating with the WCA as high as  $169^\circ$ . Kokare et al.<sup>[14]</sup> was used the ODS-modified TiO<sub>2</sub> nanoparticles to prepare hydrophobic coating on glass substrates through simple sol-gel and dip coating technique with WCA higher than  $150^\circ$ . The prepared coatings were stable against water jet impact and showed repellent towards colored and muddy water, however, the coatings were still opaque with densely white color. Despite all of the advances innovation in this field, a transparent hydrophobic surface is still greatly limited. Moreover, the use of organic solvents on the preparation of sol solution is not environmental friendly.<sup>[15]</sup> Also, the acidic nature of the sol solutions limits the choice of substrates, especially for the corrosive substrates.<sup>[16]</sup> Therefore, it is challenging to develop a simple, green approach, stable and low-cost procedure for fabricating transparent hydrophobic coating.

In this work, we demonstrated a simple, green approach and low-temperature strategy for fabricating transparent and low adhesion ultrahydrophobic coatings. The fabrication process includes two steps: (i) chemical deposition of stable and transparent TiO<sub>2</sub> films on glass substrates through a combination of peroxo sol-gel method and dip-coating technique, followed by low thermal annealing (ii) dipping modification with ODTS. The effect of surface roughness and ODTS concentration on wettability and transparency was investigated

[a] N. Pratiwi, Dr. Zulhadjri, Prof. Dr. S. Arief, Dr. D. V. Wellia  
Department of Chemistry, Faculty of Mathematics and Natural Sciences,  
Universitas Andalas, 25163, Indonesia  
E-mail: nandadiana@sci.unand.ac.id

Supporting information for this article is available on the WWW under  
<https://doi.org/10.1002/slct.201904153>

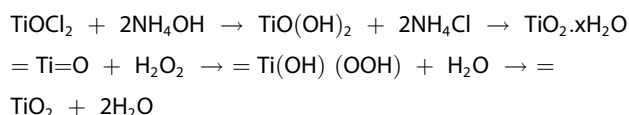
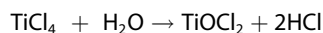


to obtain optimum parameters of fabricating transparent ultrahydrophobic surface.

## 2. Results and Discussion

### 2.1. Synthesis of TiO<sub>2</sub> Film

TiO<sub>2</sub> films were synthesized by peroxo sol-gel method, which the primary reaction equilibrium during the synthesis process of the TiO<sub>2</sub> precursors are as follows:<sup>[15,17–19]</sup>



### 2.2. Surface Morphology of TiO<sub>2</sub> thin Film

A typical TiO<sub>2</sub>-coated glass is shown in Figure 1. The coated glass is visually transparent, uniform and appears slightly yellow due to a thin film of peroxotitanium complex (PTC) solution coated on the surface (Figure 1a). The SEM image (Figure 1b) reveals that the as-prepared TiO<sub>2</sub> thin films have no cracks due to the reaction between the hydroxyl group (OH-) from PTC solution (Ti(OH)(OOH)) with ≡SiOH from pre-treated glass slide resulting in uniform coating.<sup>[15]</sup> Figure 1c shows the EDS spectra of the TiO<sub>2</sub>-coated glass. It is known that the characterized sample contains titanium and oxygen elements. Furthermore, the EDS spectrum confirms the presence of TiO<sub>2</sub>

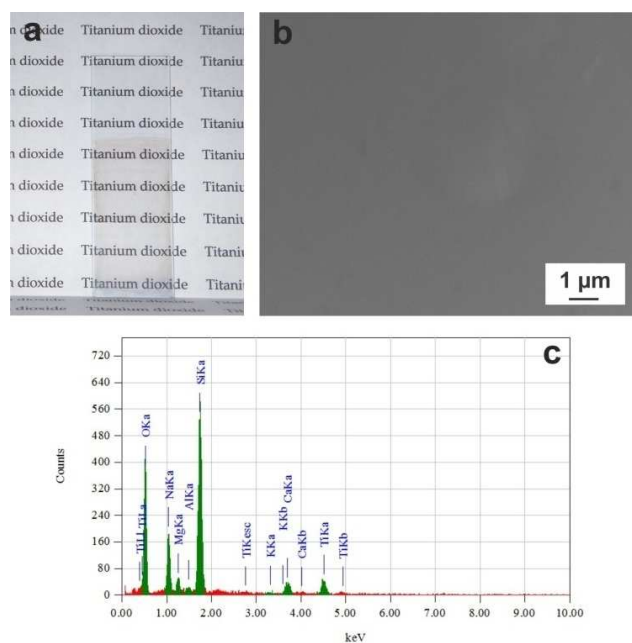


**Figure 1.** (a) photograph of transparent and uniform TiO<sub>2</sub> coated glass, (b) SEM image and (c) EDS spectra of TiO<sub>2</sub> film.

compounds on the treated glass surface. Meanwhile, the composition of other chemical elements such as Si, Ca, K, Mg, Al, and Na that detected, are derived from the sodalime glass.<sup>[20]</sup>

Figure 2(a–c) displays the AFM 3D image of untreated glass and TiO<sub>2</sub> coated glass with and without calcination treatment. It can be seen that TiO<sub>2</sub> coated glass non calcination (TNC) has a rougher surface compared to untreated glass and TiO<sub>2</sub> coated glass with calcination (TC), with the roughness parameter (Sa) are 2 nm, 3 nm and 5 nm for untreated glass, TC and TNC, respectively. The previous studies have reported that the increased surface roughness of the TiO<sub>2</sub> layer which is synthesized by using TiCl<sub>4</sub> precursors in water solvents can be obtained at the amorphous phase transition temperature to crystals. Meanwhile, the calcined TiO<sub>2</sub> layer at a temperature of 350–650 °C (temperature found in the rutile and anatase phase) has a tendency to homogenize the particles that are on its surface and further result in a decrease in surface roughness.<sup>[21,22]</sup> Therefore, the TNC was selected as the best coating to control the roughness and transparency, and used further in this study.

### 2.3. Grafting ODS

ODTS, a self-assembled monolayer molecule, has been widely used to decrease the surface energy of artificial hydrophobic surface in various substrates. The grafting mechanism that occurs during the silanization process in this study is shown in Figure 3, which begins with the physical absorption of the active ODS head group on the surface of the TiO<sub>2</sub>-coated glass. Then, hydrolysis reactions occur to form a silanol group –Si(OH)<sub>3</sub> among the active head group (–SiCl<sub>3</sub>) of ODS. Afterward, the Si-OH group from –Si(OH)<sub>3</sub> condenses with the OH group on the surface of TiO<sub>2</sub> coated glass to form covalent bonds, causing the ODS molecule to be firmly attached to the surface of the glass substrate.<sup>[23,24]</sup> Finally, condensation reactions occur among the adjacent ODS molecules, forming a cross-linked chain and a uniform densely long chain alkyl group (–C<sub>18</sub>H<sub>37</sub>), which decreases the surface energy of the TiO<sub>2</sub>-coated glass.<sup>[23,25]</sup>

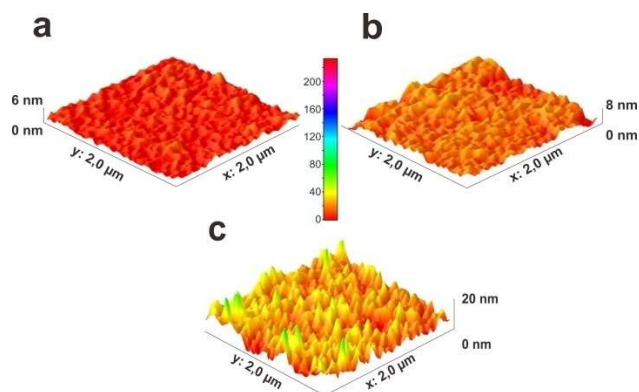


**Figure 2.** AFM images of (a) untreated glass, (b) TC and (c) TNC.

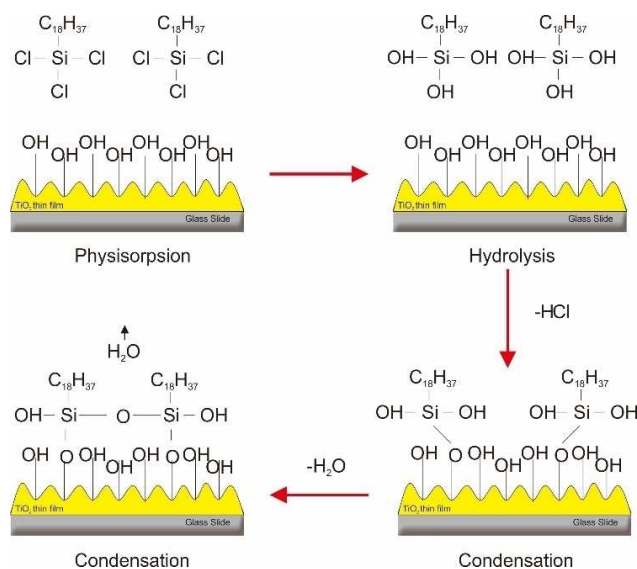


Figure 3. Schematic illustration for ODTS grafting on the  $\text{TiO}_2$  coated glass.

The wettability of the surface of the  $\text{TiO}_2$ /ODTS coated glass is greatly influenced by the concentration of the ODTS solution. Table 1 shows the static WCA and sliding angle (SA) values that obtained from all variations of the synthesized sample. Based on the results of contact angle measurements, it can be seen that the WCA value and hydrophobicity of the treated glass is increased with increasing the ODTS concentration. The lowest

Table 1. The static water and sliding angle of the sample with different ODTS concentration			
Sample	ODTS concentration (% v/v)	WCA ( $^\circ$ )	SA ( $^\circ$ )
Glass slide	0	53	45
TNC	0	65	> 50
TNC-O5	0.5	99 <sup>[a]</sup>	13
TNC-O1	1	103	8
TNC-O15	1.5	146	7

TNC-O15 means that concentration of ODTS = 1.5 %. [a] water droplet did not remain constant

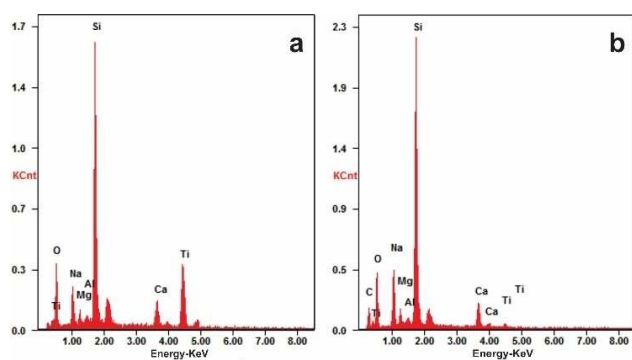


Figure 4. EDS spectrum of (a) TNC and (b) TNC-O15.

water contact angle value of the treated glass in the presence of ODTS was obtained at an ODTS concentration of 0.5 %, with a WCA of  $99^\circ$  and continues to increase until it reaches the ultrahydrophobic surface at an ODTS concentration of 1.5 % with a WCA of  $146^\circ$ . In opposite, the SA values of the treated glass are decreased with increasing the ODTS concentration. The lower SA value indicated the dynamically ultrahydrophobic surface that can be used for the water-repellent or self-cleaning surface application.<sup>[26]</sup>

## 2.4. Chemical Composition of Coating Surface

Figure 4(a-b) shows a typical EDS spectra of the  $\text{TiO}_2$  coated glass (TNC) and  $\text{TiO}_2$ /ODTS coated glass (TNC-O15). As shown in Figure 4a, the EDS spectra of the TNC shows a high intensity of Ti and O spectrum. The element of Si, Na, Mg Al and Ca are originates from the sodalime glass slide. However, after the  $\text{TiO}_2$ -coated glass being modified with ODTS, the high intensity of Si and C elements were detected, followed by a decrease of Ti and O elements. This result confirms that the ODTS molecules have been successfully grafted onto the  $\text{TiO}_2$  layer (Figure 4b).

## 2.5. FTIR Analysis

FTIR characterization was used to confirm the presence of ODTS and its interactions on the surface of the  $\text{TiO}_2$ -coated glass after chemical modification. Figure 5 shows the FTIR spectrum of  $\text{TiO}_2$  coated glass (TNC) and  $\text{TiO}_2$ /ODTS coated glass (TNC-O15) in the range of  $4000\text{--}400\text{ cm}^{-1}$ . The spectra of TNC shows a wide absorption band at  $900\text{--}950\text{ cm}^{-1}$ , which is attributed to the Si-O-Ti stretching vibration (Figure 5a). This result confirms that  $\text{TiO}_2$  film was coated on the surface of sodalime glass.<sup>[27,28]</sup> After the  $\text{TiO}_2$  coated glass being modified with ODTS, a new absorption band was observed at  $1025\text{ cm}^{-1}$ , which is assigned to asymmetric Si-O-Si stretching vibration

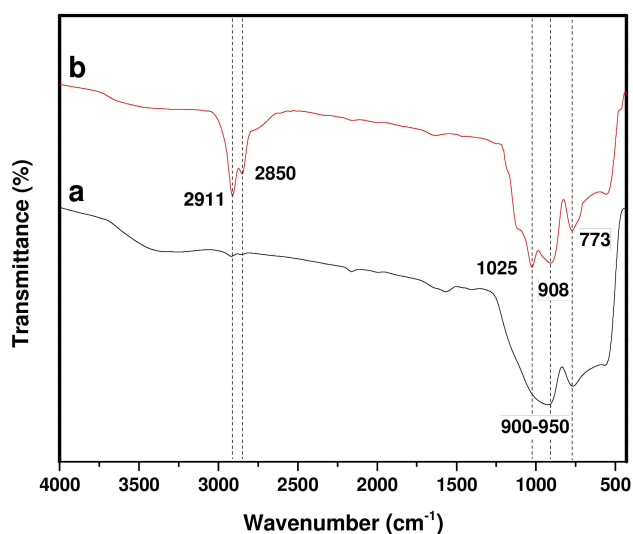
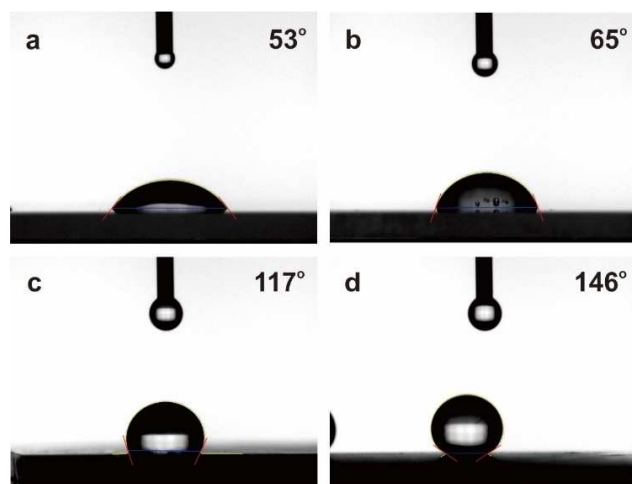


Figure 5. FTIR spectra of (a) TNC and (b) TNC-O15.

(Figure 5b). This absorption band occurs as a result of the cross-linked interaction of ODTs on the ultrahydrophobic glass.<sup>[27,29]</sup> In addition, the absorption band at around  $908\text{ cm}^{-1}$ , which is observed in the spectrum of TNC–O15, is assigned to the stretching vibration of Si–O–Ti. This result can be attributed to the interaction between Si–OH groups found in the head of ODTs with the Ti–OH group from the condensed  $\text{TiO}_2$  layer, forming Si–O–Ti interaction by releasing water molecules.<sup>[30,31]</sup> The absorption bands at about  $2911\text{ cm}^{-1}$  and  $2850\text{ cm}^{-1}$ , which is only observed in the TNC–O15, are attributed to asymmetrical and symmetrical (C–H) stretching vibrations, respectively (Figure 5b).<sup>[13,31,32]</sup> This absorption band confirms the presence of long chain alkyl groups from ODTs compounds.<sup>[31,32]</sup> Besides, the FTIR spectra of TNC and TNC–O15 show absorption band at  $773\text{ cm}^{-1}$  correspondings to Si–O–Si symmetric stretching vibration of sodalime glass.<sup>[33]</sup>

## 2.6. Wettability

It has been demonstrated that the wettability of solid surface not only involves surface roughness, but also relates to the modification with low-surface-energy material.<sup>[12]</sup> In the present case, the deposition of  $\text{TiO}_2$  films on the glass surface could provide the surface topography for the ultrahydrophobicity. However, nanostructured  $\text{TiO}_2$  itself is a hydrophilic material ( $\text{WCA} < 90^\circ$ ).<sup>[34]</sup> To reduce the surface energy, the hydrophilic  $\text{TiO}_2$ -coated glass (TNC) was treated with low-surface-energy ODTs by the dipping method. Figure 6 shows the images of static water drops on the untreated glass,  $\text{TiO}_2$  coating before and after ODTs modification, respectively. Both the untreated glass and the TNC display hydrophilic nature (Figure 6a and b), and the treated glass slide with monolayer ODTs of 1.5% (O-15) shows the hydrophobic property with a WCA of  $117^\circ$  (Figure 6c). However, the  $\text{TiO}_2$ -coated glass slide with subsequent hydrophobic treatment presents remarkably increased ultrahydrophobicity with a static water contact angle as high as  $146^\circ$  (Figure 6d). In conclusion, with the combination of  $\text{TiO}_2$



**Figure 6.** Images of water droplets on (a) untreated glass, (b) TNC, (c) O-15 and (d) TNC–O15.

films creating high surface roughness and the ODTs monolayer lowering the surface energy, a large amount of air is trapped into the interspaces or cavities of the ultrahydrophobic glass, and the water droplet is primarily connected with the trapped air.<sup>[10,35]</sup> Therefore, the treated glass cannot be wetted by a water droplet and presents ultrahydrophobicity.

## 2.7. Self-Cleaning Property

In order to evaluate the self-cleaning property of the as-prepared ultrahydrophobic surface, we spread carbon particles (64 mesh) as dust onto the surface. Figure 7 displays the process of the self-cleaning effect of the untreated glass and TNC–O15, which was recorded by a digital camera. The carbon particles were placed on the surface of ultrahydrophobic glass (TNC–O15), and the contaminated surface was then rinsed with water. As shown in Figure 7a–d, the carbon particles on the surface of TNC–O15 were easily removed by rolling of water droplets, resulting in a spotless surface. However, the carbon particles on the untreated glass were tremendously difficult to clean in a similar procedure (Figure 7e–h). Besides, the self-cleaning ability of ultrahydrophobic glass against refined sands as a real contaminant was also evaluated (Figure S1). The surface of the as-prepared ultrahydrophobic glass (TNC–O15), as expected, was able to completely removed the refined sands after rinsing with water. Therefore, it can be concluded that the ultrahydrophobic surface can protect glass substrate from the dust accumulation in practical applications.

## 3. Conclusions

In summary, a facile and straightforward method was successfully developed to fabricate transparent ultrahydrophobic coatings through depositing  $\text{TiO}_2$  film on glass substrate, followed by low thermal annealing and surface modification with ODTs. The stable and transparent  $\text{TiO}_2$  layer that synthesized through the peroxo sol-gel method, was able to increase the surface roughness for trapping air. Meanwhile, the ODTs monolayer with concentration of 1.5% (v/v) was able to decrease the surface energy of the roughened surface producing transparent ultrahydrophobic glass with WCA of  $146^\circ$  and SA of  $7^\circ$ , which also showed excellent self-cleaning performance compared to untreated glass. Moreover, this facile method not only offering

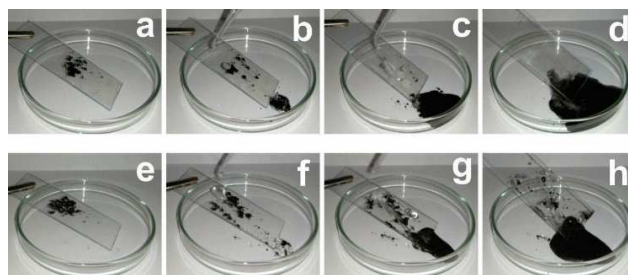


**Figure 7.** Self-cleaning phenomena of the (a–d) TNC–O15 and (e–h) untreated glass.

an effective strategy but also promising large scale applications for manufacturing ultrahydrophobic surfaces in both industrial and scientific fields.

### Supporting Information Summary

Experimental procedures and additional data are provided in the Supporting Information.

### Acknowledgements

The authors acknowledge Universitas Andalas for financial support (contract number: T/58/UN.16.17/PP.IS.KRP2GB/LPPM/2019).

**Keywords:** Octadecyltrichlorosilane • self-cleaning • TiO<sub>2</sub> • transparent • ultrahydrophobic glass

- [1] Y. Y. Quan, L. Z. Zhang, *Sol. Energy Mater. Sol. Cells* **2017**, *160*, 382–389.
- [2] Z. Zuo, J. Gao, R. Liao, X. Zhao, Y. Yuan, *Mater. Lett.* **2019**, *239*, 48–51.
- [3] S. Sutha, S. Suresh, B. Raj, K. R. Ravi, *Sol. Energy Mater. Sol. Cells* **2017**, *165*, 128–137.
- [4] T. Kamegawa, Y. Shimizu, H. Yamashita, *Adv. Mater.* **2012**, *24*, 3697–3700.
- [5] T. Kamegawa, K. Irikawa, H. Yamashita, *Sci. Rep.* **2017**, *7*, 13628.
- [6] I. P. Parkin, R. G. Palgrave, *J. Mater. Chem.* **2005**, *15*, 1689–1695.
- [7] Y. Wang, B. Li, T. Liu, C. Xu, Z. Ge, *Colloids Surf. A* **2014**, *441*, 298–305.
- [8] C. W. Extrand, S. I. Moon, *Langmuir* **2014**, *30*, 8791–8797.
- [9] M. Zhang, S. Feng, L. Wang, Y. Zheng, *Biotypologie* **2016**, *5*, 31–43.
- [10] C.-H. Xue, S.-T. Jia, J. Zhang, J.-Z. Ma, *Sci. Technol. Adv. Mater.* **2010**, *11*, 33002.
- [11] Y. Rahmawan, L. Xu, S. Yang, *J. Mater. Chem. A* **2013**, *1*, 2955–2969.
- [12] Y. Wang, B. Li, T. Liu, C. Xu, Z. Ge, *Colloids Surf. A* **2014**, *441*, 298–305.
- [13] A. Syafiq, A. K. Pandey, V. Balakrishnan, N. A. Rahim, *Pigment Resin Technol.* **2018**.
- [14] A. M. Kokare, R. S. Sutar, S. G. Deshmukh, R. Xing, S. Liu, S. S. Latthe, *AIP Conf. Proc.*, American Institute Of Physics, **2018**, p. 100068.
- [15] Q. C. Xu, D. V. Wellia, R. Amal, D. W. Liao, S. C. J. Loo, T. T. Y. Tan, *Nanoscale* **2010**, *2*, 1122–1127.
- [16] N. Sasirekha, B. Rajesh, Y. W. Chen, *Thin Solid Films* **2009**, *518*, 43–48.
- [17] H. Ichinose, M. Terasaki, H. Katsuki, *J. Ceram. Soc. Jpn.* **1996**, *104*, 715–718.
- [18] J.-K. Park, H.-K. Kim, *Bull. Korean Chem. Soc.* **2002**, *23*, 745–748.
- [19] S. Il Seok, M. Vithal, J. A. Chang, *J. Colloid Interface Sci.* **2010**, *346*, 66–71.
- [20] A. E. Adeoye, E. Ajenifuja, B. A. Taleatu, A. Y. Fasasi, *J. Mater.* **2015**, *2015*, 1–8.
- [21] J. Aarik, A. Aidla, T. Uustare, V. Sammelselg, *J. Cryst. Growth* **1995**, *148*, 268–275.
- [22] W. Chiappim, G. E. Testoni, J. S. B. de Lima, H. S. Medeiros, R. S. Pessoa, K. G. Grigorov, L. Vieira, H. S. Maciel, *Braz. Inst. Agron. Nordeste Bol. Tec.* **2016**, *46*, 56–69.
- [23] J. Liu, X. Zhu, H. Zhang, F. Wu, B. Wei, Q. Chang, *Colloids Surf. A* **2018**, *553*, 509–514.
- [24] K. S. Kim, J. H. Kim, H. J. Lee, S. R. Lee, *J. Mech. Sci. Technol.* **2010**, *24*, 5–12.
- [25] B. Xu, Z. Cai, *Appl. Surf. Sci.* **2008**, *254*, 5899–5904.
- [26] A. S. K. Topcu, E. Erdogan, U. Cengiz, *Colloid Polym. Sci.* **2018**, *296*, 1523–1532.
- [27] M. Mokhtarimehr, M. Pakshir, A. Eshaghi, M. H. Shariat, *Thin Solid Films* **2013**, *532*, 123–126.
- [28] S. Miranda, A. Vilanova, T. Lopes, A. Mendes, *RSC Adv.* **2017**, *7*, 29665–29671.
- [29] Y. Hendrix, A. Lazaro, Q. L. Yu, H. J. H. Brouwers, *J. Photochem. Photobiol. A* **2019**, *371*, 25–32.
- [30] V. Purcar, V. Rădițoiu, A. Dumitru, C. A. Nicolae, A. N. Frone, M. Anastasescu, A. Rădițoiu, M. F. Raduly, R. A. Gabor, S. Căprărescu, *Appl. Surf. Sci.* **2019**, *487*, 819–824.
- [31] A. A. Widati, N. Nuryono, I. Kartini, *AIMS Mater. Sci.* **2019**, *6*, 10–24.
- [32] H. Li, N. Li, Y. Zhang, H. He, Z. Liu, *J. Sol-Gel Sci. Technol.* **2017**, *83*, 518–526.
- [33] M. Torres-Carrasco, J. G. Palomo, F. Puertas, *Mater. Constr.* **2014**, *64*, 1–14.
- [34] J. Medina-valtierra, M. Sánchez-cárdenas, C. Frausto-reyes, S. Calixto, *J. Mex. Chem. Soc.* **2006**, *50*, 8–13.
- [35] J. T. Simpson, S. R. Hunter, T. Aytug, *Reports Prog. Phys.* **2015**, *78*, 086501.

Submitted: November 1, 2019

Accepted: January 8, 2020